PHILOSOPHICAL TRANSACTIONS OF THE ROYAL SOCIETY B BIOLOGICAL SCIENCES

Experimentally Determined Microcracking around a Circular Hole in a Flat Plate of Bone: Comparison with Predicted Stresses

P. Zioupos, J. D. Currey, M. S. Mirza and D. C. Barton

Phil. Trans. R. Soc. Lond. B 1995 **347**, 383-396
doi: 10.1098/rstb.1995.0031

Experimentally determined microcracking around a circular hole in a flat plate of bone: comparison with predicted stresses

P. ZIOUPOS[1], J. D. CURREY[1], M. S. MIRZA[2] AND D. C. BARTON[2]

[1] *Department of Biology, The University of York, York YO1 5DD, U.K.*
[2] *Department of Mechanical Engineering, The University of Leeds, Leeds LS2 9JT, U.K.*

SUMMARY

We examined the microcracking (damage) in the vicinity of a circular hole in bovine femoral bone specimens. The stresses near the hole were derived by a finite element analysis model using the bone's elastic constants and yield stresses, which were determined from a series of mechanical tests specifically for the type of bone under examination. The spatial occurrence and distribution of microcracking was compared to the patterns of the predicted maximum principal stress, the von Mises stress, and the strain energy density function (all implicated by various workers as stimuli for bone remodelling) and to the predictions derived by the use of two engineering criteria for anisotropic yield under mixed mode of stress. The predictions for stresses and the strain energy density were all very similar, making it impossible to claim that any of them is superior to the others. However, empirical examination of the results of the Hencky-von Mises and Tsai-Wu anisotropic yield criteria showed that the Tsai-Wu criterion approximated reasonably the pattern of microcracking around the hole. We suggest that, in the light of the considerable damage observed in the vicinity of stress concentrators, similar damage in irregular material interfaces (i.e. near orthopaedic implants) would require the re-examination of the theories concerning bone remodelling so as to account for the possibility of occurrence of damage and the quantification of its magnitude and likely effect. The presence of considerable microdamage in bone long before it fails suggests that damage-based criteria are more likely to be successful predictors of bone remodelling behaviour than would stress or strain-based criteria.

1. INTRODUCTION

Many aspects of the fracture of bone, particularly those related to fracture in the micro- and meso-mechanical level, are poorly understood. If strongly loaded, bone experiences damage in the form of microcracking (Zioupos & Currey 1994) and the onset of this microcracking coincides with the appearance of a region of 'yield' in the stress/strain curve. *In vivo* such microdamage is constantly repaired and healed by the process of remodelling (Frost 1960; Martin & Burr 1989). *In vitro*, bones of different mineralization levels and structures demonstrate different modes of damage (Zioupos *et al.* 1994). By examining a variety of mineralized tissues serving different functional needs, one can gain a better insight into the failure mechanisms of bone. For instance, studies of specimens made of nearly unidirectional mineralized fibres from the dentine of the tusk of the Narwhal *Monodon monoceros* showed that the mechanics of mineralized lamellae can be described by continuum theories (Currey *et al.* 1994). The bone of antlers, which are relatively lightly mineralized, shows very characteristic micromechanical modes of failure involving the lamellae of its osteons (Zioupos *et al.* 1994) whereas the more highly mineralized bovine bone behaves more like a continuum material. The extent to which the widely applied engineering continuum theories (of deformation and failure) are suitable for bone as a whole is as yet very unclear, and for modelling purposes such theories need to be reassessed.

There are two reasons why it is important to have an understanding of these damage phenomena in bone. One is that it will allow us to predict more precisely the situations in which bone will or will not crack and then fail. This is likely to be particularly important in the consideration of the possible failure of bone near prostheses, where the stress situation is both complex and unnatural. The other reason is that there is intense interest at the moment in finding the algorithms that could be used to allow bone cells to remodel adaptively, and damage may be one of the processes to which bone reacts in modelling and remodelling.

Bone is able to respond to varying functional needs by modelling, which involves a changing of shape and/or size, and remodelling, which involves turnover of existing bone (Frost 1973; Currey 1984). The function of modelling is easy to understand. The function of remodelling is not so clear; presumably in some way it acts to improve the quality of the bone material. Many algorithms have been produced that seem to produce (in a computer) what looks like

Phil. Trans. R. Soc. Lond. B (1995) **347**, 383–396
Printed in Great Britain

adaptive modelling and remodelling (Cowin 1993; Huiskes & Hollister 1993). These algorithms are based on various guesses regarding the mechanical stimulus that is responsible for the (re)modelling (modelling and/or remodelling) process. There are two main approaches. The first assumes that (re)modelling occurs in response to the state of stress or strain in the bone, either: (i) the level of the local strain energy density (Huiskes *et al.* 1993); (ii) the level of the distortional energy (Carter *et al.* 1991; Van der Meulen *et al.* 1993; Mittlmeier *et al.* 1994); (iii) the level of principal strain (Firoozbakhsh & Cowin 1981; Frost 1983; Turner *et al.* 1994); or (iv) the 'energy stress', derived from the local strain energy density (Fyhrie & Carter 1986, 1990; Carter *et al.* 1989). There are other candidate algorithms. The second approach assumes that damage is in some way the stimulus, either: (i) some form of fatigue damage or some variant of it (Carter *et al.* 1987) or; (ii) the accumulated damage that occurs when the rate of damage generation is not equal to the rate of damage repair (Prendergast *et al.* 1993; Prendergast & Taylor 1994). Not all authors assert that the bone cells actually measure these properties, rather, the bone models seem to respond correctly if these properties of the state of the bone were measured and responded to.

The mechanical measures of the first (stress or strain-based) approach are only applicable in the absence of damage and would yield erroneous results if applied to damaged bone. In the presence of damage mechanical measures (i.e. stress, strain) take 'effective' values. For instance, as microcracking (Zioupos & Currey 1994) reduces the load bearing area the actual magnitude of stress ('effective' stress) increases. Algorithms based on these effective values have not appeared yet: the reason for this is perhaps the lack of methods for the quantification of the magnitude of damage locally. If there is bone (re)modelling in response to cracking, an efficient criterion for the (re)modelling process must be the one related to the way in which microcracking in bone actually happens.

We have used finite element analysis to examine the pattern of stresses around holes in bone, using three different ways of characterising the stresses, and compared these patterns with the pattern of microcracking observed directly by a microscopical method.

For the finite element analysis we needed the elastic constants (moduli of elasticity and the Poisson's ratio values) of our material to derive the distribution of stresses and strains around the hole. We determined experimentally the angular variation of elastic and ultimate properties. Furthermore, we also needed yield functions to describe what might be expected to be the spatial distribution of the microcracks, whose relation to the distribution of stress and strain is not obvious. We make use of two engineering criteria for anisotropic yield and compare their predictions to the actual occurrence of microcracks.

2. MATERIALS AND METHODS

About 70 specimens were cut from the diaphysis of two bovine femurs from an animal aged about 18 months. At that age the bone is not completely mineralized, and so its elastic moduli are somewhat less than some other values found in the literature. We did not take specimens from the posterior region underneath the areas of muscle insertion. (This region is intensely remodelled in femurs.) We define three anatomical orientations in bone: 'longitudinal' from end to end, 'radial' across the bone's thickness, and 'tangential' at right angles to the two previous directions. Bone is in general anisotropic between these three directions; its macroscopic/textural mechanical properties are those of an 'orthotropic' or a 'transversely isotropic' material (Reilly & Burstein 1974; Katz & Meunier 1987; Cowin & Mehrabadi 1989).

(*a*) *Mechanical tests*

All mechanical tests were performed in an INSTRON 1122 universal testing machine at about 20 °C, either in a water bath or under constant water irrigation. 'Nominal stress' σ (load divided by the initial cross sectional area) was used for the stress values at yield and 'engineering strain' ϵ (derived from the movement of the grips) was used to calculate the tangent modulus of elasticity of the initial linear region. Account was taken of the compliance of the machine and the grips, and the calculated moduli of elasticity were effectively the same as those derived from the use of a contact extensometer, which was used occasionally to verify the results.

(*i*) *Tensile tests*

The angular behaviour of the elastic constants, and the stresses at yield, was examined by tensile tests. Thirty dumb-bell-coupon shaped specimens (total length 60 mm, reduced central section length 22 mm, width 4 mm, thickness 2 mm, shoulders 5 mm radius) were cut at various angles over a 0–90° range (the 0° direction being the longitudinal one), on the bone's longitudinal/tangential plane, the samples' length and width also lying on the longitudinal/tangential plane. The specimens were thinned down to approximately 1.5 mm using progressively finer grades of carborundum paper. Tension tests to failure were carried out at a cross head speed of 2 mm min^{-1}, which for a gauge length of 22 mm resulted in a nominal strain rate of 0.0015 s^{-1}.

(*ii*) *Compression tests*

Compression tests were performed on 20 cubes of bone of sides $5 \times 5 \times 5$ mm oriented along the three principal directions. A single compression loading to destruction was performed on each cube along one of the principal directions (seven longitudinal, seven radial, six tangential). The cross head speed was 1 mm min^{-1}, which resulted in a nominal strain rate of 0.0034 s^{-1}. Due to the occasional slightly non-uniform contact of the bone with the compressive platens at the ends, the strain values of these tests are not always entirely reliable. However, in these experiments we were primarily interested in recording the ultimate loads (and consequently stresses) that the bone could

PHILOSOPHICAL TRANSACTIONS OF THE ROYAL SOCIETY B BIOLOGICAL SCIENCES

sustain and therefore these problems do not matter much.

(*iii*) *Poisson's ratio tests*

For the measurement of the Poisson's ratio nine specimens were cut as prismatic bars 40–50 mm long with a 5×5 mm square section. Four specimens had their long direction along the longitudinal direction and five specimens were in the tangential direction of the bone. The specimens were cycled three times in tension in the linear elastic region. During each stretch an extensometer was used to measure successively the longitudinal extension and the lateral contractions in the two normal directions. The ratios of the σ/ϵ slopes, measured on the screen of an oscilloscope, were used to provide the Poisson's ratio values.

(*b*) *Microscopical observations*

(*i*) *Preparation and loading*

The remaining specimens were coupon shaped, approximately 50 mm long, 7 mm wide and 2 mm thick. Holes of diameters in the range of 500–800 μm were drilled, and the specimens were subsequently thinned to a final thickness of 1.5 mm with progressively finer grades of carborundum paper. Specimens for microscopy needed a mirror finish, which was produced with a Buehler Micropolish (0.05 μm gamma alumina) powder. During the whole preparation the specimens were immersed in water. They were then cycled a number of times while immersed in a fluorescein solution (Zioupos & Currey 1994) in the INSTRON (nominal strain rates in the range of $[2 \times 10^{-4}$–$10^{-3}\ s^{-1}]$ to an ever higher load at each cycle, until a deviation from linearity was evident in the load/deformation curve. A note was made of the highest stress level attained; the load was returned to zero and the samples were removed for microscopic inspection.

(*ii*) *Microscopy*

Images of microcracking around the holes were obtained by the use of a BIO-RAD 600 Series Laser Scanning Confocal (LSC) system and work station, using a krypton/argon mixed-gas laser which emits strongly at 488, 568 and 647 nm. The LSC system was attached to a NIKON Diaphot Inverted Fluorescence microscope. The data were stored in optical disks and were visualized, analysed and processed by use of the 'Thru-View ©' software. Copies of black/white or pseudocoloured images were produced by a Sony UP 5000P video printer. This microscopic facility has a number of advantages. First, the laser light is tuned to the excitation level of the fluorophore dye (fluorescein, 490 nm) and thus one can achieve excellent contrast between the site of the dye molecules and the background (unstained) intensity level. Second, the laser source provides monochromatic light of small divergence, high brightness and high degree of spatial resolution. Third, the confocal mode can focus on a spot at a defined level inside the specimen and by a scanning action produce a thin inner section of the specimen on a z-plane. A three-dimensional image of the cracks can be built by focusing at different z-depths, while the clarity of imaging of the cracks can be further enhanced by software routines on the workstation (Zioupos & Currey 1994).

(*c*) *Analysis*

For bone under uniform tension we have observed that the occurrence of microcracking coincides with the appearance of 'macroscopic' (as opposed to 'microscopic', which is at smaller stresses (Bonfield & Datta 1974)) yield in the σ/ϵ curve and also the departure from linear behaviour. The onset of microcracking has been confirmed by both microscopic observations (Zioupos & Currey 1994) and acoustic emission studies (Zioupos *et al.* 1994) and for the well mineralized bovine bones occurs in the region of 100 MPa, which is considerably higher than any stress encountered during physiological loading *in vivo* (Rubin *et al.* 1990). The observation of microcracks by our method is limited to a depth of at most 300 μm from any free surface. There are two main reasons for this depth limitation: (*i*) the dye penetrates from the surface and it takes time to fill the new spaces and; (*ii*) bone is naturally translucent, not transparent, and its mineral in particular is able to attenuate the laser beam rapidly. However, the size of our samples is small and therefore, we can access a significant amount of the microcracked volume of the material. We have no indications that what we see from the surface is not typical of the processes occurring elsewhere in the samples.

An aim of the present study is to examine whether the pattern of microcracking, caused by a mixed mode of stress in the vicinity of a hole, can be reasonably predicted. In two previous studies (Hayes & Wright 1977; Cezayirlioglu *et al.* 1985) two engineering criteria emerged as likely candidates for anisotropic yield in bone (see Appendix 1). Cezayirlioglu *et al.* (1985) suggested that both the Hill (1948) and the Tsai-Wu (1971) criteria were particularly able to describe the anisotropic and macroscopic yield behaviour of bone specimens that had been subjected to a combination of uniform tension and torque along their axial (longitudinal) direction. Because our specimens are thin we examined the two-dimensional case. Instead of the original Hill (1948) criterion we use the Hencky-von Mises one (Fisher 1967), this is a later, improved, form of the Hill criterion in that it includes a term for the interaction between the two normal directions. It gives a yield function:

$$k(\sigma_x, \sigma_y \tau_{xy}) = (\sigma_x/X_t)^2 + (\sigma_y/Y_t)^2 + (\tau_{xy}/S)^2 - K(\sigma_x \sigma_y/X_t Y_t), \quad (1a)$$

where: $$K = [E_x(1+\nu_{yx}) + E_y(1+\nu_{xy})]/2[E_x E_y(1+\nu_{xy})(1+\nu_{yx})]^{1/2}. \quad (1b)$$

$k(\sigma_x, \sigma_y, \tau_{xy})$ is a function of the stresses along x and y the two main directions, x is always in the direction of tension, y is transversely to the latter on the plane of the

PHILOSOPHICAL TRANSACTIONS OF THE ROYAL SOCIETY B BIOLOGICAL SCIENCES

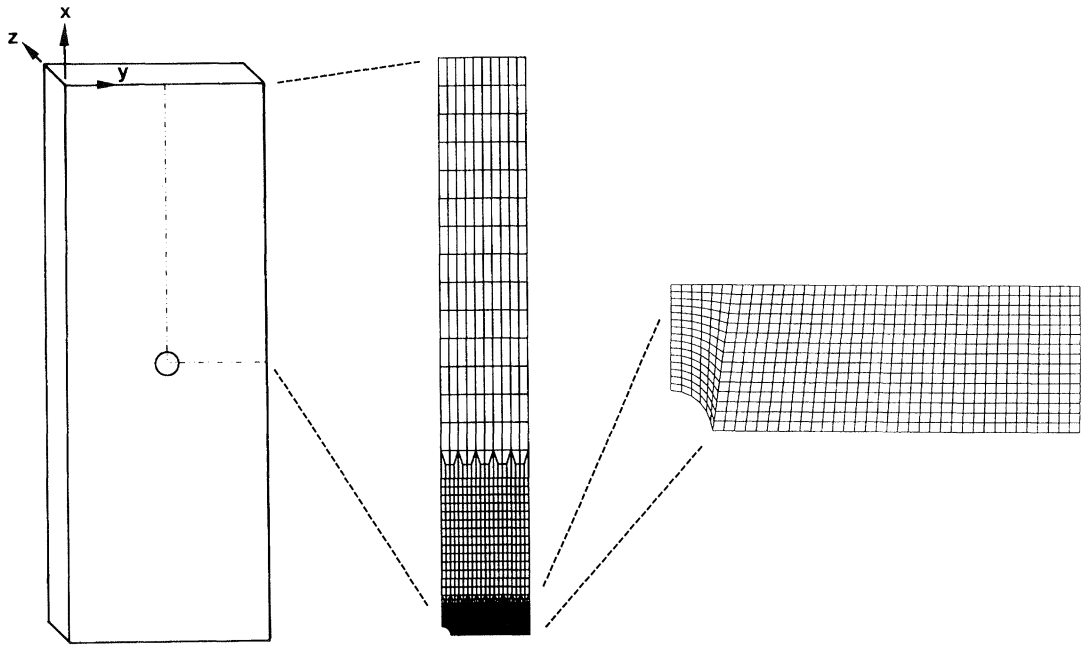

Figure 1. (*a*) the geometry of the bone specimens; (*b*) the FEA mesh covering a quarter of the bone specimen; (*c*) results will be presented for this denser segment of the mesh nearer the hole where stresses vary considerably.

specimen; X, Y, S are yield stresses; we use t for tension and c for compression (where appropriate); E_i $(i = x, y)$ are the moduli of elasticity; $\nu_{ij} = -\epsilon_j/\epsilon_i$ is the Poisson's ratio due to uniaxial stress applied in the i-th direction; σ_i $(i = x, y)$ the normal stresses and τ_{ij} the shear stress.

This is a distortional energy criterion, which is used routinely for composite materials (Newaz & Majumdar 1992). The main drawback of the criterion is that it assumes yield in tension and compression to occur at the same stress, which is not in general the case and certainly not for bone (Reilly & Burstein 1975).

The second criterion is that of Tsai & Wu (1971):

$$f(\sigma_x, \sigma_y, \tau_{xy}) = F_x\sigma_x + F_y\sigma_y + F_{xx}\sigma_x^2 + F_{yy}\sigma_y^2 + F_{xy}\sigma_x\sigma_y + F_{ss}\tau_{xy}^2$$

where $F_x = (X_c - X_t/X_c X_t)$, $F_y = (Y_c - Y_t/Y_c Y_t)$,

$$F_{xx} = (1/X_c X_t), \quad F_{yy} = (1/Y_c Y_t),$$

$$F_{xy} = 1/(X_c X_t Y_x Y_t)^{1/2}, \quad F_{ss} = (1/S^2).$$

The same notation as previously used applies here. This criterion results from a strength tensor theory and, although the coefficients F_{ij} can be specified as functions of the yield stresses by using a variety of test modes, the general tensorial expression of the criterion was again a postulate by Tsai & Wu. The linear terms of σ_i it incorporates allow for differences in yield in tension and compression. The cross terms $\sigma_i\sigma_j$ allow for interactions between stress components. At the expense of more complexity and an increased number of parameters the Tsai-Wu promises to provide a more accurate description of composite yield data (Hayes & Wright 1977).

Both criteria postulate that a material under a combination of stresses shows yield when the mathematical functions $k(\sigma_x, \sigma_y, \tau_{xy})$ or $f(\sigma_x, \sigma_y, \tau_{xy})$ reach the value of 1. The arithmetic values of functions $k(\sigma_x, \sigma_y, \tau_{xy}), f(\sigma_x, \sigma_y, \tau_{xy})$ change with the site in the vicinity of a stress concentrator, and we utilize this feature to provide us with a map of the region yielded by microcracking.

(*d*) *Finite element model*

A prediction of the stresses around the machined holes was derived using the finite element method. The implicit two-dimensional code NIKE2D developed by Lawrence Livermore National Laboratory, University of California was employed for this purpose. Because our samples are thin, plane stress conditions were specified, and an orthotropic elasticity option was used to model the anisotropic properties of the sample. This gives the constitutive matrix in terms of the orthogonal material axes, a and b, as follows:

$$C^{-1} = \begin{bmatrix} 1/E_a & -\nu_{ba}/E_b & -\nu_{ca}/E_c & 0 \\ -\nu_{ab}/E_a & 1/E_b & -\nu_{cb}/E_c & 0 \\ -\nu_{ac}/E_a & -\nu_{bc}/E_b & 1/E_c & 0 \\ 0 & 0 & 0 & G_{ab} \end{bmatrix}, \quad (3)$$

where E_i is the elastic modulus in the i-th direction; ν_{ij} is the Poisson's ratio; G_{ab} is the shear modulus in the ab plane. Directions a, b and c are the material properties directions; the bone's material properties along the anatomical directions: 1:radial, 2:tangential and 3:longitudinal can be placed along a, b & c in a number of ways. One has then to define the angle between the abc system of axes and the xyz system of axes, which defines the direction of tensile stresses.

PHILOSOPHICAL TRANSACTIONS OF THE ROYAL SOCIETY B BIOLOGICAL SCIENCES

Values of the constants were incorporated from the results of the mechanical tests described above. Due to symmetry, only 1/4 of the entire specimen was modelled, using, typically, 1100 four-noded isoparametric elements as indicated in figure 1*b*. The mesh was denser in the vicinity of the hole and we present here only the behaviour of a smaller segment of the mesh of 600 elements (see figure 1*c*). Appropriate boundary conditions were applied along the planes of symmetry and the tensile load was applied uniformly across the free end of the specimen.

NIKE2D predicts the direct stresses σ_x and σ_y and the in-plane shear τ_{xy} at four Gauss points in each element of the model for the imposed loading conditions. These stresses were read and the strain energy density (SED):

$$\text{SED} = (1/2)\,[\sigma_x \epsilon_x + \sigma_y \epsilon_y + \tau_{xy} \epsilon_{xy}] \qquad (4)$$

and the values of the yield functions according to equations 1 and 2 computed. The spatial variation of these values was then indicated on contour plots. Note that because the analysis was purely elastic, predicted values for the functions $k(\sigma_x, \sigma_y, \tau_{xy}), f(\sigma_x, \sigma_y, \tau_{xy})$ can exceed unity. An anisotropic elastic-plastic analysis would be required to ensure more realistically that $k(\sigma_x, \sigma_y, \tau_{xy}),\ f(\sigma_x, \sigma_y, \tau_{xy}) \leqslant 1$. We shall also be examining the patterns of the maximum principal stress ($\sigma_{\max}$) and the von Mises stress (σ_{VM}). In order for the contours to be roughly similar to those of the yield functions we show the versions of $\sigma_{\max}$, σ_{VM} and SED normalized by their maximum values.

3. RESULTS

(*a*) *Elastic constants and yield stresses of bone*

In this section we derive the material properties of our bovine bone (unnotched undamaged samples). The uniaxial tensile behaviour of our femoral bone varied regularly with the direction between 0° and 90°. Figure 2 shows typical σ/ϵ curves in tension and compression at 0° and 90°. The main features were similar to those reported in the literature (see review by Viano 1986): bone was stronger in compression than in tension; the 0° direction was both stiffer and stronger than the 90° one in both tension and compression. Different samples (of different geometry) were used for tension and compression and therefore we can not be categorical that the moduli of elasticity for tension and compression were equal. However, by cycling some of our tensile bone specimens within the linear elastic region in tension and compression we found that the σ/ϵ curve passed through the origin with unchanged slope, a result also found previously by Reilly *et al.* (1974). Therefore we consider for the purpose of our analysis that the moduli of elasticity in tension and compression for a particular specimen are the same.

Figure 3*a* shows the angular variation of the modulus of elasticity between the longitudinal and tangential directions in a bovine femur. There was a gradual decline between the stiff longitudinal direction and the tangential direction, which was about half as stiff. There was considerable variability, probably caused mostly by variations associated with different positions along the diaphysis of the femur. We noticed, for instance, that the middle of the femur was stiffer and more anisotropic than bone towards the metaphysis. Pope & Outwater (1974) and Lotz *et al.* (1991) report similar findings. The continuous line is the least squares regression based on the rule of transformation of elastic constants between these two normal directions. It can be used to provide an estimate of the modulus in shear (G) on the longitudinal/tangential plane of the tissue (Currey *et al.* 1994).

Yield stresses also showed a systematic and regular decline between the main directions (figure 3*b*). Both the Hencky-von Mises and the Tsai-Wu criteria can be used to describe the angular variation of this *macroscopic* yield for whole samples. A least squares best fit was produced by using the Hencky-von Mises criterion. This gave yield stresses of 78.8 MPa in the 0° direction and 28.2 MPa in the 90° direction, and also gave an estimate for the in-plane yield stress in shear, S of 35 MPa. A least squares fit using the Tsai-Wu criterion, with values for yield in compression given by the compression tests, produced an estimate of $S =$ 74 MPa. However, there is very little difference between the two criteria in the tensile quadrant. In the presence of compressive stresses only the Tsai-Wu criterion is able to describe the behaviour by using one set of material constants.

(*b*) *Microcracking around holes in bone samples*

From the same femur we chose: (i) a typical stiff sample (number 54), which was stretched to a maximum nominal stress of 96 MPa along its 'stiff' direction; (ii) a softer specimen (number 11), from near the proximal end of the femur (where other experiments showed us the bone was more isotropic), which was also stretched along its 'stiff' direction to a maximum nominal stress of 60 MPa; and (iii) a typically stiff diaphyseal specimen (number 12), which was stretched to a maximum nominal stress of 36 MPa along its 'compliant', tangential direction. Table 1 summarizes the results for the elastic constants and the yield stresses for three specimens, which we use to demonstrate the application of our analysis. The elastic modulus of the three specimens was measured before the holes were drilled. The other properties for each specimen shown in table 1 were obtained by knowing the general relation between these variables (derived in the large series of tests for other specimens) and by then scaling them according to their longitudinal elastic modulus. Table 1 also includes the values (or estimates) given in two other studies of the angular dependency of the elastic and ultimate properties of bone (Reilly & Burstein 1975; Cezayirlioglu *et al.* 1985). Reilly & Burstein (1975) concentrated their efforts on the ultimate characteristics of bone, consequently the data they gave for anisotropic yield were incomplete and we have filled in table 1 with what we estimate would be reasonable estimates of the stresses at yield for their kind of bone. On the other hand Cezayirlioglu *et al.* (1985) did not report the moduli of elasticity for their specimens, which would have allowed us to scale the

PHILOSOPHICAL TRANSACTIONS OF THE ROYAL SOCIETY B BIOLOGICAL SCIENCES

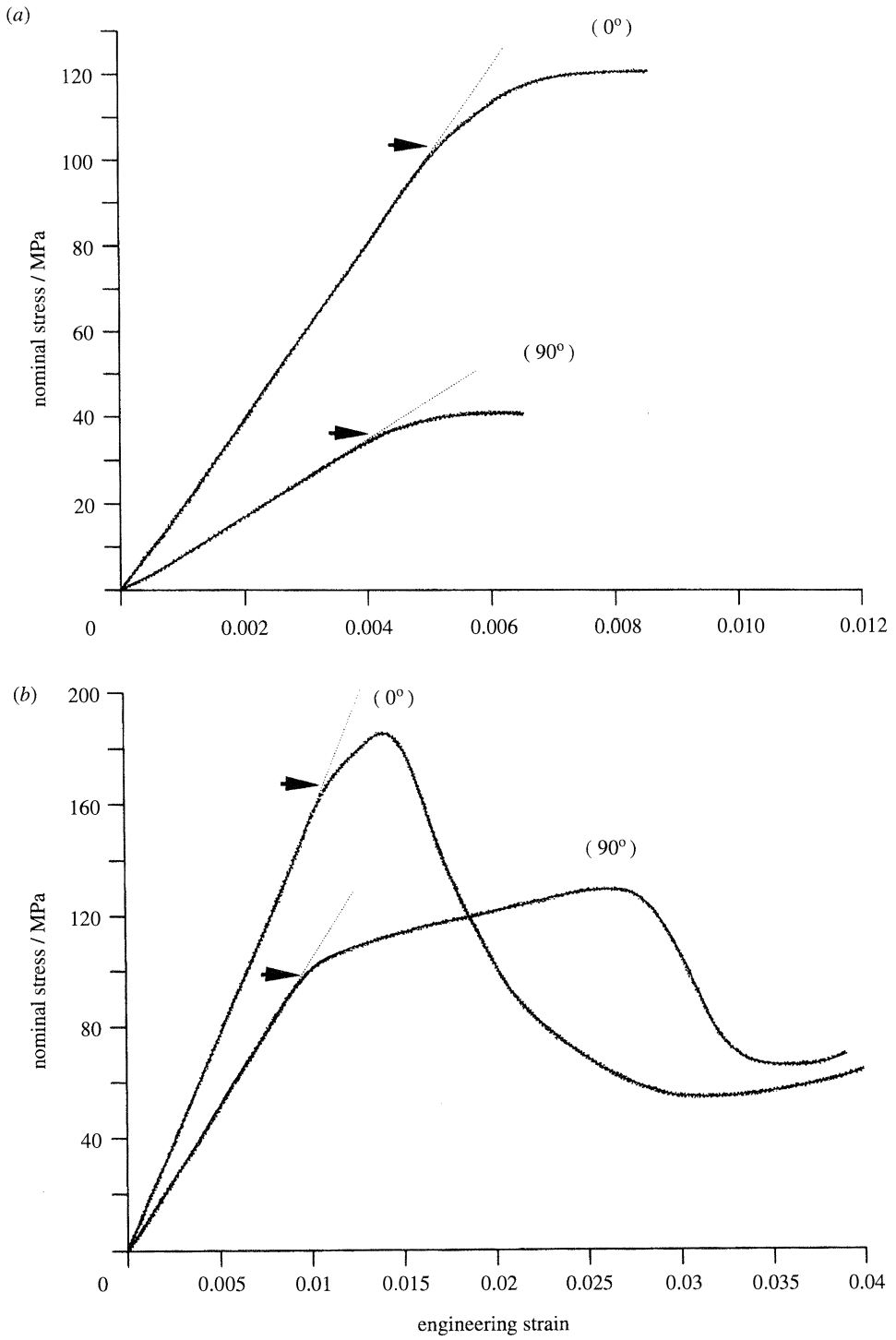

Figure 2. (*a*) typical simple stress/strain (σ/ϵ) tension curves for two bone (unnotched, undamaged) specimens orientated along the longitudinal (0°) and tangential (90°) directions. Microcracking starts at the level where there are signs of macroscopic yield and a noticeable deviation from linearity (arrows); (*b*) σ/ϵ curves in compression along the same directions for two other bone specimens (also unnotched, undamaged). Note the difference in scale of the strain axis between tension and compression. The behaviour in tension and compression was very similar up to the point of the maximum sustainable load, the behaviour of bone in compression after that point is, for the present purposes, irrelevant.

yield stresses to the actual stiffness of our specimens. Moreover, Cezayirlioglu *et al.* (1985): (i) were concerned mainly with the axial (longitudinal) properties and therefore their report and treatment for the transverse properties of bone is incomplete; and also (ii) instead of reporting the actual yield stresses they gave their values in the form of the F_{ij} coefficients of the Tsai-Wu function or the other criteria they investigated. This would have been all right if functions F_{ij} were in fact invariant with the type of bone, but it is evident from table 1 that F_{ij} vary considerably for the different types of bone. The approach of Cezayirlioglu *et al.* (1985) utilises only three coefficients F_{ij} and a specific pattern of stresses, which is also only applicable along the bone's stiff longitudinal direction (compare their coefficients with those for specimen 12 in table 1).

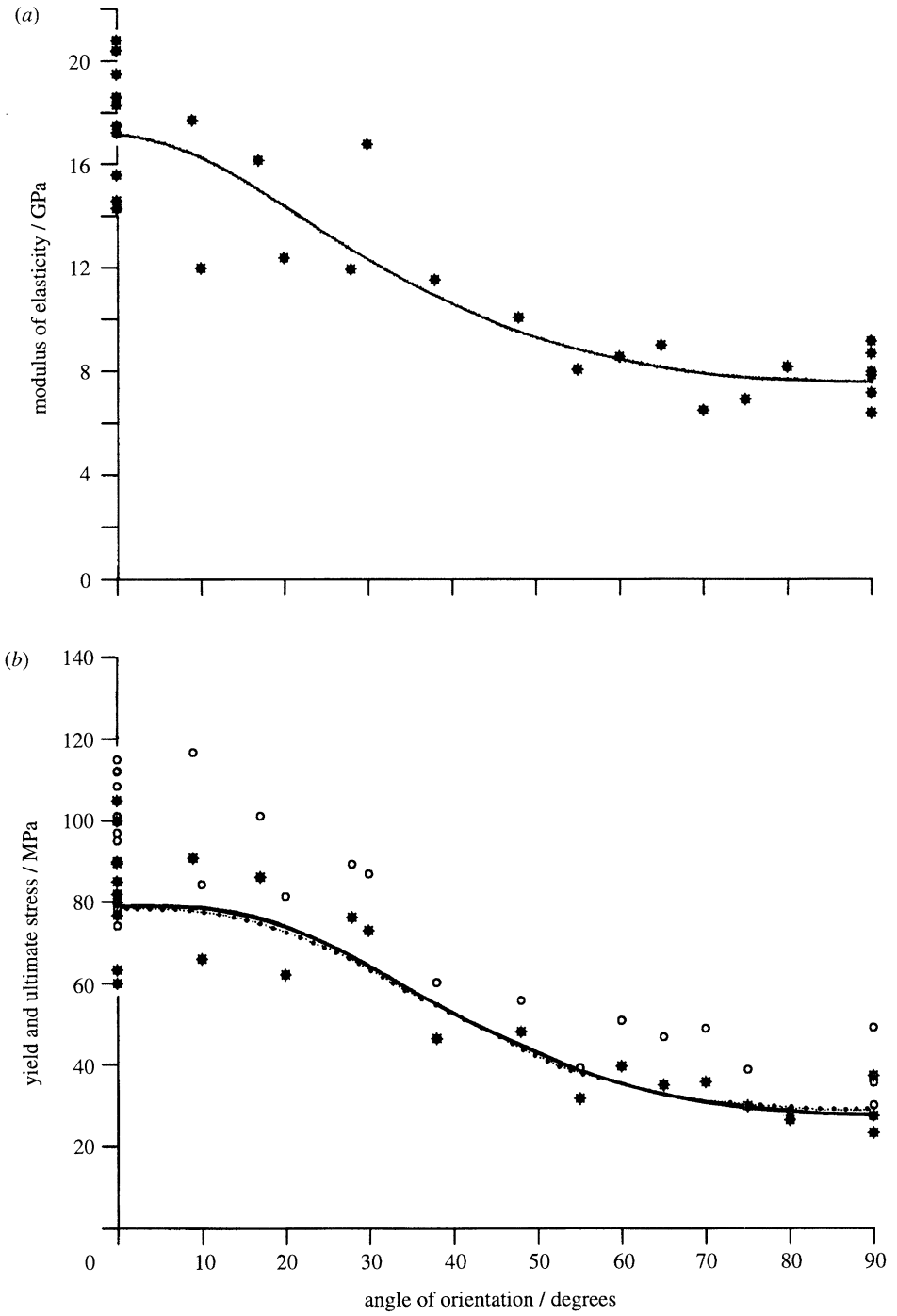

Figure 3. (*a*) the angular variation of the modulus of elasticity of bovine bone between the longitudinal (0°) and tangential directions (90°), the smooth curve is drawn by use of the rule of transformation of the elastic constants with the angle of orientation; (*b*) the angular variation of the occurrence of macroscopic yield (stars) observed for bovine bone specimens (unnotched, undamaged), the smooth line is the prediction by using equation 1 and the dotted line by using equation 2, * denotes yield, ○ denotes ultimate: the angular variation of the ultimate tensile stress (○) is shown but these data are not used in the present study.

Figures 4*a*, 5*a* and 6*a* show the pattern of microcracking that developed around the hole in the three bone specimens and also the FEA modelled for each of five situations: the first principal stress, the von Mises stress, the SED, the Hencky-von Mises criterion and the Tsai-Wu criterion. For the analysis only one quadrant is needed because of the elastic symmetry around the centre of the hole. We give a qualitative description of the distribution of the stresses, the yield criteria, and the microcracking in table 2.

Figures 4*b*, 5*b* and 6*b* show the pattern of the first maximum (most tensile) principal stress. Its magnitude is maximum at 90° on the equator, where it is tensile, and is orientated along the *x*-axis. At the pole (0°) only the second principal stress is present; it is compressive and lies along the *y*-axis. The reason for considering the maximum principal stress is that there is evidence (Zioupos & Currey 1994) that cracks in bone at the microscale level develop mostly normal to the tensile field. However, what is also apparent is that the

Table 1. *The elastic constants and yield stresses used in the* FEA *examination of the microcracking pattern of three femoral samples (numbers 54, 11, 12) and similar values given in two sources in the literature*

(Directions: 1-radial, 2-tangential, 3-longitudinal. Stress axes: *x*-tension, *y*-transverse in the plane of the specimen, *z*-transverse across the thickness. t, tension; c, compression.)

	specimen number				
	54	11	12	Reilly & Burstein (1975)	Cezayirlioglu *et al.* (1985)
elastic constants					
E_3/GPa	18.3	13.1	20.0	22.3–26.5	—
$E_1 \approx E_2$/GPa	8.80	9.35	9.50	10.0–12.0	—
G/GPa	4.50	3.08	4.92	3.57–5.09	—
$\nu_{32} \approx \nu_{31}$	0.350	0.330	0.350	0.29–0.41	—
$\nu_{23} \approx \nu_{13}$	0.168	0.235	0.165	(0.11–0.17)[a]	—
ν_{12}	0.430	0.430	0.430	0.44–0.51	—
yield stresses/MPa					
X_t	100.5	72.0	38.0	140–141	132
Y_t	35.7	38.0	110.0	(35–40)[a]	—
S	49.2	33.7	53.6	(< 68)[a]	57
X_c	171.1	157	137.0	(< 210)[a]	196
Y_c	131.1	136	177.0	(< 150)[a]	—
Tsai-Wu coefficients					
$F_x/10^{-3} \times \mathrm{MPa}^{-1}$	4.1	7.5	19.0	2.3[a]	2.5
$F_{xx}/10^{-5} \times \mathrm{MPa}^{-2}$	5.8	8.9	19.2	3.4[a]	3.9
$F_{ss}/10^{-4} \times \mathrm{MPa}^{-2}$	4.1	8.8	3.5	2.8[a]	3.1
$F_y/10^{-2} \times \mathrm{MPa}^{-1}$	2.0	1.9	0.34	1.9[a]	—[b]
$F_{yy}/10^{-4} \times \mathrm{MPa}^{-2}$	2.1	1.9	0.51	1.8[a]	—[b]
$F_{xy}/10^{-4} \times \mathrm{MPa}^{-2}$	1.1	1.3	0.99	0.8[a]	—[b]

[a] Denotes an estimated value.

[b] Invalid for this application of the Tsai-Wu criterion; also note that two out of the three remaining coefficients are an order of magnitude different from those for specimen 12.

microcracks soon interact with the anisotropy of the material and their orientation tends to incline overall towards the weaker tangential direction (see figure 6*a*).

The *in vivo* study of Brown *et al.* (1990) showed that the first principal stress was the measure which correlated most closely in the short term (four weeks) to the remodelling response of the turkey bone tissue. In the longer term (eight weeks) other measures like the SED, the dilatational stress and the longitudinal shear stress also showed satisfactory correlations. Our observations and the study by Brown *et al.* (1990) suggest the possibility that the early remodelling, which seems to be related to the first principal stress, may prevent the onset of microcracking.

Figures 4*c*, 5*c*, 6*c* show the contours for the von Mises stress. The values of the von Mises stress are necessarily increased nearer the 45° direction because of the contribution of the shear stresses (see Appendix 2). However, this is a step in the wrong direction since the best measure would predict the predominance of microcracks at 0°. We consider the von Mises stress here because it has been implicated by some (Carter *et al.* 1991; Mittlmeier *et al.* 1994) as a (re)modelling mechanical stimulus on the assumption that the tissue responds to distortional, rather than to dilatational stresses. Shear-slip cracks are associated with ductile, non-brittle materials. Although at the microscale bone develops cracks in a brittle manner, bone is not very brittle at the macroscale. This is a consequence of microcracking in that a larger material volume containing microcracks behaves as a continuum exhibiting post-yield deformation, which looks like 'plasticity'. On the other hand the very presence of microcracks in the vicinity of stress concentrators has a beneficial effect by 'blunting' sharp flaws and shielding inhomogeneities.

Figures 4*d*, 5*d*, 6*d* show the contours for the strain energy density (SED) around the hole. This measure includes dilation as well as distortion and is considered by some to be the most likely candidate for a (re)modelling stimulus in bone (Huiskes & Hollister 1993). It shows maximum values at the equator (where most cracks developed in all three of our samples). The magnitude of the SED declines much more rapidly than with the other criteria, but this is to be expected since, in SED, the stresses are in effect squared. If bone (re)models according the SED pattern, the (re)modelling process would have some effect in averting some of these cracks. Because SED includes both deviatoric (distortional) and hydrostatic (dilatational) modes of stress the underlying similarities in the contours of figures 4, 5, 6 (part *cs*) and figures 4, 5, 6 (part *ds*) are not surprising. Use of the von Mises or SED-based stimuli gives very similar results in (re)modelling studies of bones in the literature, therefore on the basis of the outcome one can not decide which of the two is preferable. Some workers assigned a specific (re)modelling potential to the distortional part of the SED and a potential for bone resorption to the dilatational part of the SED (Carter 1987; Carter & Wong 1988). Cowin (1990) pointed out that for the isotropic linearly elastic FEA models

PHILOSOPHICAL TRANSACTIONS OF THE ROYAL SOCIETY B BIOLOGICAL SCIENCES

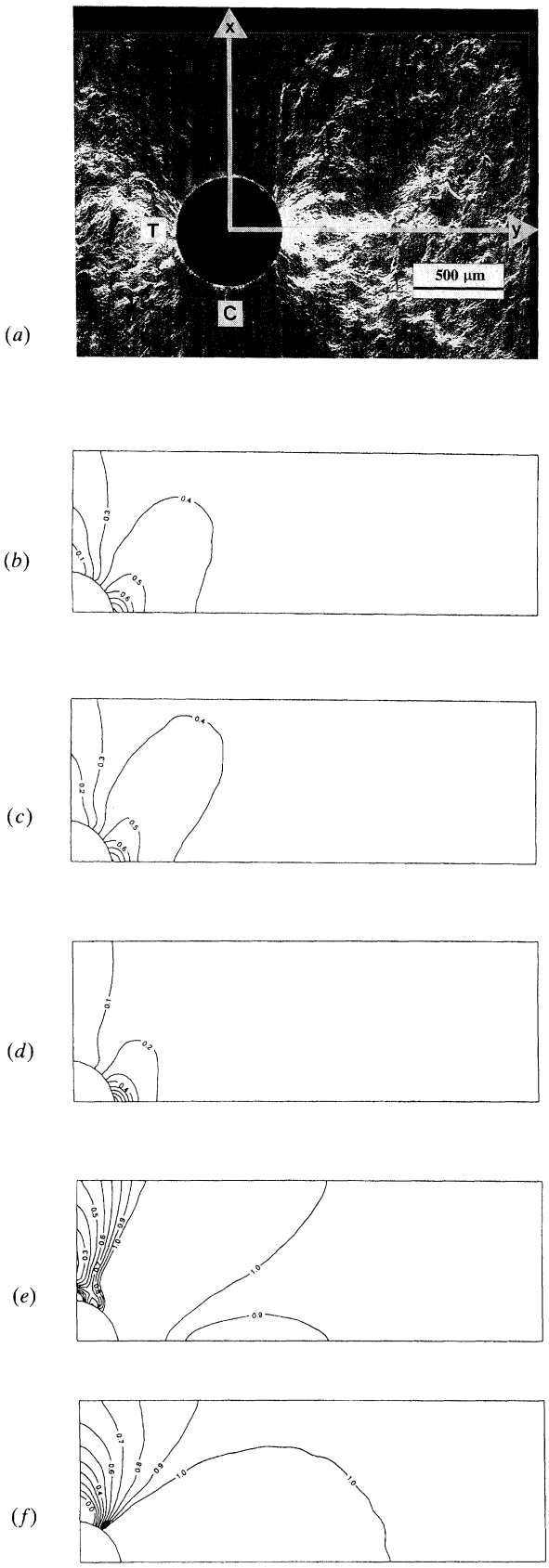

Figure 4. (*a*) microcracking around a 550 μm diameter hole in specimen number 54; tension is applied in the *x*-direction. Microcracks appear readily in regions under tension (T) compared to regions under compression (C). (*b*) pattern of normalized maximum principal stress: (*c*) pattern of normalized von Mises stress; (*d*) pattern of normalized SED; (*e*) yield contours for the Hencky-von Mises criterion; (*f*) yield contours for the Tsai-Wu criterion. The yield contours of value 1 are in effect a boundary where the material starts to yield; no account is taken of the fact that because of the yield, the original elastic stress may be redistributed and retransmitted.

that all workers use in the literature the separation is easy, but for anisotropic elastic materials (like bone in nature and our present application) the two components (distortional and dilatational) are in fact coupled to each other and the separation is more complicated.

The contour plots of maximum principal stress, von Mises, and Strain Energy Density do differ to some extent. But these differences are not marked enough to produce differences in remodelling behaviour great enough to distinguish between them as the effective remodelling signal.

The bottom two insets in figures 4, 5 and 6 are the predictions produced by the two failure criteria. Figures 4*e*, 5*e*, 6*e* show the pattern of microcracking as predicted by the Hencky-von Mises criterion (equation 1). It fails in general to predict the large amount of microcracking at the equator, instead it predicts that most microcracking happens in a 'butterfly' pattern (at 45°) where maximum shear stresses occur. This pattern is produced by the distortional nature of the criterion and the fact that provision is not made for different yield stresses in tension and in compression. This difference is, however, used in the predictions produced by the Tsai-Wu criterion (figures 4*f*, 5*f*, 6*f*) which predicts consistently a failure zone concentrated at the equator.

5. DISCUSSION

(*a*) *Microcracking in bone*

Throughout the years a small number of workers (Frost 1960; Tschantz & Rutishauser 1967; Currey & Brear 1974; Martin & Burr 1989) reported what seemed to be rather scant and inconclusive evidence of cracking in bone. However, lately by the use of *en bloc* staining in either fluorescein (compact bone: Zioupos & Currey 1994) or fuchsin (cancellous bone: Fyhrie & Schaffler 1994) the characterization of microcracks shorter than 100 μm has been made possible. Fyhrie & Schaffler (1994) suggested that 'matrix' microdamage in bone trabeculae had two main failure modes, both caused by shear stresses.

The trabeculae are slender and therefore they either bend or buckle. Trabeculae along the compressive direction either split or crack in cross-hatched mode; trabeculae at right angles to the stress fracture completely. Compact bone, by comparison, showed what Zioupos & Currey (1994) called 'structural' microdamage. These were cracks within the compact body of the tissue, which also related to the mode of stresses (or strains). No single mode of stress could be identified as a universal cause of damage and these workers suggested that microcracks developed according to the local combination of stresses. Therefore the quest for engineering criteria to describe the pattern of microcracking is very important.

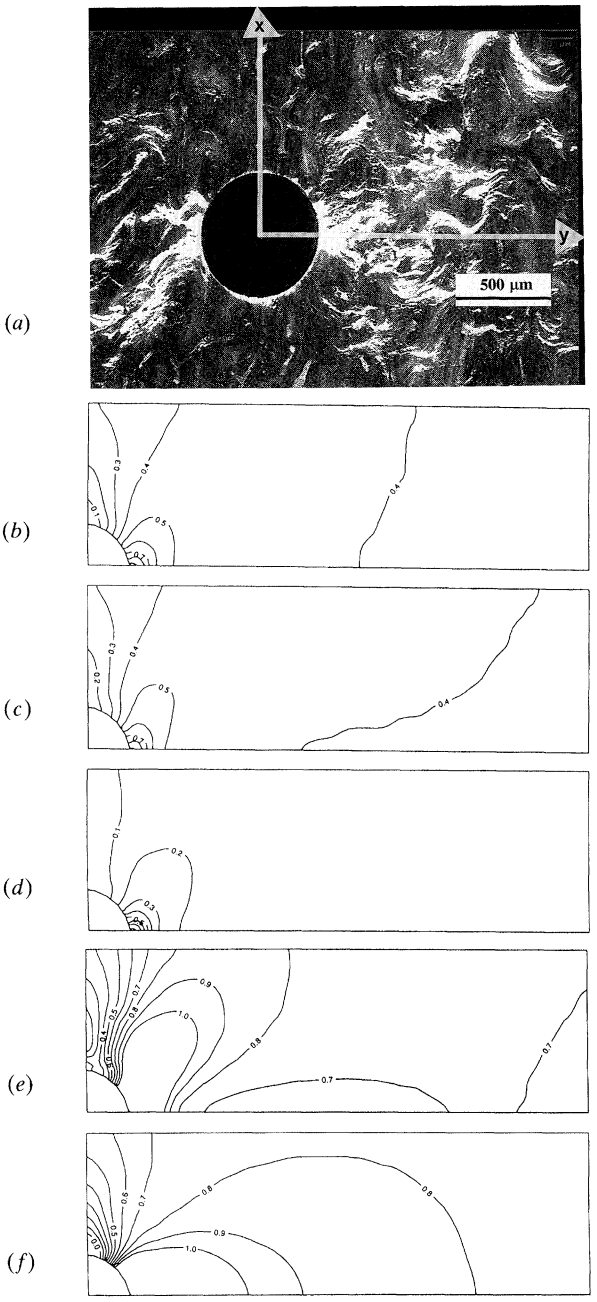

Figure 5. (*a*) microcracking around a 550 µm diameter hole in specimen number 11; (*b*) pattern of normalized maximum principal stress; (*c*) pattern of normalized von Mises stress; (*d*) pattern of normalized SED; (*e*) yield contours for the Hencky-von Mises criterion; (*f*) yield contours for the Tsai-Wu criterion.

At this point we have to make a distinction. Most of the rather bigger cracks observed by various workers (Frost 1960; Tschantz & Rutishauser 1967; Martin & Burr 1989; Mori & Burr 1993) as a result of loading *in vivo* were either induced exogenously or were observed in aged animals. The present study addresses the question of induced microcracking *in vitro* in healthy younger bones. Our bovine bone was completely free of microcracks caused from the everyday activity of the animal and our study does not intend to extrapolate into normal physiological conditions. However, when microcracking is present for whatever reasons (stress concentrations, ageing, insertion of implant devices) one wishes to know the pattern for its development.

We have examined here the microcracking pattern that developed near a circular hole. This geometric inhomogeneity was simple enough to model confidently by FEA methods and allowed us to compare the occurrence of the cracks in relation to some candidate remodelling criteria and two engineering criteria for anisotropic yield. In compact bone shear stresses were not the dominant generators of microcracks; this was evident from the absence of a 'butterfly' pattern in the holes around the 45° direction. However, the shear strength of bone is presumably direction dependent (Saha 1977) and there are at least two microscopic studies (Mori & Burr 1993; Zioupos & Currey 1994) where microcracks were readily created by longitudinal shear. On the other hand, it seems that tensile stresses of a magnitude that exceeds the yield stress for compact bone were particularly capable of opening up cracks in the microscale.

The distinction between the 'microscale' and the 'macroscale' is also important. Zioupos *et al.* (1994) pointed out that the cracking in the microscale depends critically on the fine structure of the bone and on the degree of cohesion brought about by different amounts of mineralization in different bones (Currey & Brear 1992). These early microdamage events make some types of bones more brittle than others. The final outcome is, however, influenced greatly by a second stage of 'structural' microdamage, where at the macroscale microcracks form clouds, from one of which a final macrocrack develops which drives through the structure. For making predictions on the likely effect of a cloud of microcracks we need suitable continuum theories which can be easily implemented in computer simulations. The Tsai-Wu yield criterion has been shown through: (i) its application to the macroscopic behaviour of whole bone samples (Hayes & Wright 1977; Cezayirlioglu *et al.* 1985); and (ii) in the empirical comparison of its yield contours to the pattern of microcracking of our present study, to describe well the anisotropic yield behaviour of bone. We may now consider the significance of possessing such a tool for analysis.

(*b*) (*Re*)*modelling in bone*

There are some implications of this work, concerned with the (re)modelling functional adaptation processes occurring in life and also the mathematical rules that are being used by bioengineers to simulate these adaptive processes. It seems sensible to describe the functional needs of bone as lying between two extremes: (i) that having to do with incipient failure and consequently requiring (re)modelling to be a repair mechanism and; (ii) that concerned only with life on the safe side of failure and consequently needing (re)modelling as an optimisation mechanism. In most situations, of course, the distinction between these two conditions is blurred. The shape, form and material properties of bone are a result of an evolutionary process where not only strength, but also the opti-

PHILOSOPHICAL TRANSACTIONS OF THE ROYAL SOCIETY B BIOLOGICAL SCIENCES

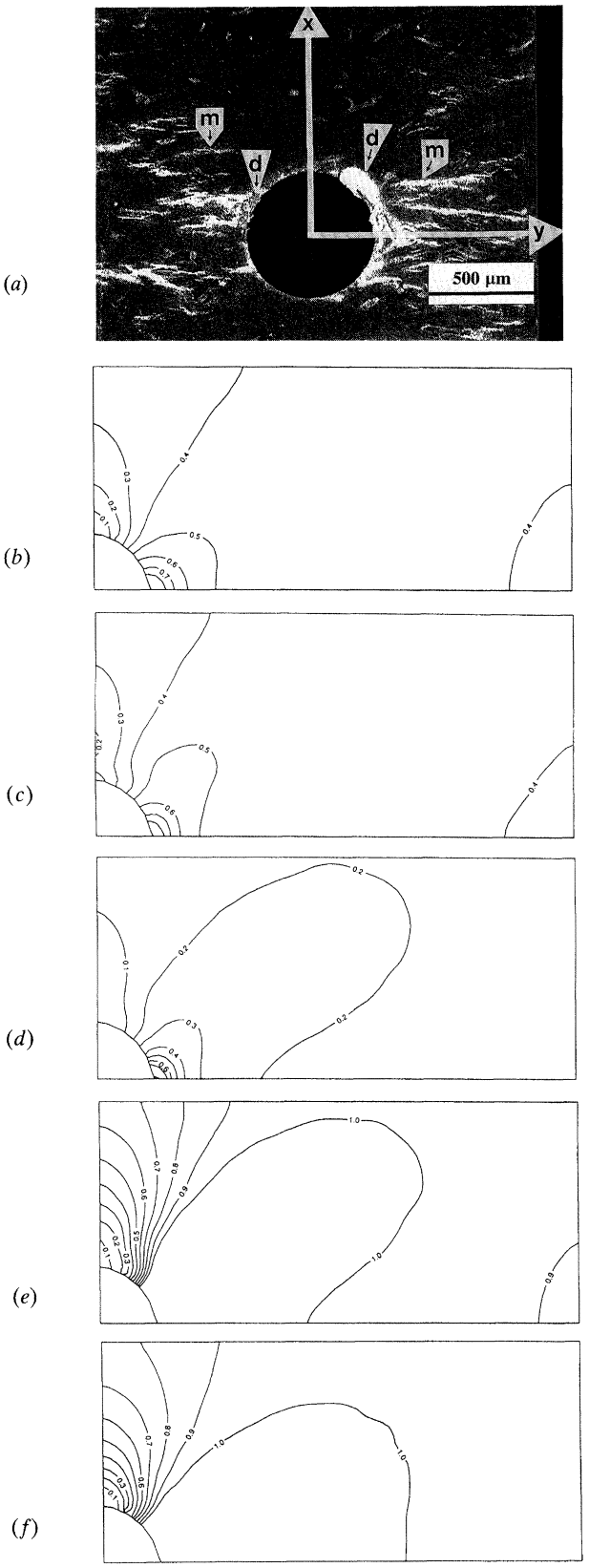

Figure 6. (*a*) microcracking around a 550 μm diameter hole in specimen number 12; (*b*) pattern of normalized maximum principal stress; (*c*) pattern of normalized von Mises stress; (*d*) pattern of normalized SED; (*e*) yield contours for the Hencky-von Mises criterion; (*f*) yield contours for the Tsai-Wu criterion. Note that at the microscale cracks (m) open mostly along the weak direction. Some damage caused by a slight eccentricity of the drill during the preparation can be seen near the hole (d).

misation between material resources, time for construction, weight, and other features are all subject to natural selection. Bones' basic designs are written in the DNA, and therefore some bones, like the auditory ossicles, or the antlers of deer, which are barely tested mechanically before they are formed, can emerge as competent forms ready for action (Currey 1984). It is unlikely therefore that stresses have a role to play in the initial formation of a bone, but it is nevertheless also certain that afterwards during ontogeny and adult life stresses (or strains) are the predominant modelling and remodelling factors (Rubin *et al.* 1990).

The question arises as to how bone's weakness is monitored and how incipient failure, or at least microcracking, plays a part in the bone's (re)modelling process. It seems reasonable to suggest that in life (re)modelling will happen (though not necessarily exclusively) as a response to local damage. Microcracking is an everyday phenomenon (Frost 1960), which is usually dealt with adequately. In such a case some of the (re)modelling 'stimuli' (such as the damage-mechanics defined 'effective' stress, or the accumulated damage) suggested by engineers are applicable throughout the whole spectrum of stresses from zero to failure. For instance, in the absence of damage 'effective stress' (Kachanov 1958) equals ordinary stress. When damage starts, 'effective stress' increases as a function of the amount of damage. Alternative predictors for remodelling could be based on the anisotropic yield criteria we have examined in the present study. However, yield criteria are scalar expressions for damage and thus in this case they can only predict the development of 'isotropic' damage within the yield boundaries. A microcrack is by its very nature 'anisotropic', and 'isotropic' damage requires cracks to be completely randomly oriented within the damaged area. In the purely elastic case, as used in our FEA programs, and effectively all others in the literature, the problem turns into how to deal with yield functions having a value greater than 1. One simple method in elastic FEA techniques would be to exclude those elements of the mesh which are at the areas that have been damaged beyond some level. This indeed would of course increase the stress in the nearby areas and by use of any of the standardly assumed mechanical stimuli would trigger (re)modelling. However, bearing in mind the directionality of both microcracks and remodelling what is really required is a directionally dependent function for the development of damage, presumably in the form of a 'damage' tensor.

The real problem is conceptual rather than analytical, however. For instance those workers who favour SED considerations or the von Mises stress, believe that because there is a stress shielding effect in bone, whereby a stiffer volume carries more stress than a nearby soft one, that therefore ultimately stiffer members get more and more stiff while softer ones get softer and eventually dissolve. Recently this method has been used to explain the formation of a cancellous structure from an initially homogeneous medium (Huiskes & Hollister 1993; Smit & Schneider 1994). However, what this implies for compact bone *in vivo* is

Table 2. *A brief description of the microcracking pattern and the behaviour of the mechanical measures*

criterion	number 54 less isotropic	number 11 more isotropic	number 12 normal to long axis
maximum principal stress	max at 90°, falling rapidly to 0.5, mid-range at 45°	as for less isotropic, but mid-range stress much broader	as for number 11
von Mises stress	max at 90°, falling rapidly to 0.5–0.7 at about 45°	as for less isotropic, but mid-range stress wider spread	as for number 11
strain energy density	max at 90°, falling rapidly to 0.2–0.7 at about 70°	as for less isotropic	as for number 11
Hencky-von Mises criterion	max at 45°, broad distribution of maximum, complex near pole	max at 45°, broadish distribution of maximum, complex near pole	max at 45°, very broad distribution of maximum, rapid decline from maximum
Tsai-Wu criterion	max at 90°, broad distribution of maximum, falling slowly to 0–0.7 at about 30°	max at 90°, broadish distribution of maximum, falls slowly to 0–0.7 at about 30°	max at 90°, very broad distribution of maximum, falling slowly to 0–0.7 at about 30°
microcracking pattern	mainly at 90° or so out to about 30°	mainly at 90° or so out to about 30°	no strong concentration at 90°, initiating from 90° to about 45°, but then travelling at 90°

that damaged areas would become more and more soft and structural failure would result. It is surely wrong for there to be a 'failure happy' mechanism which will inevitably cause failure after the appearance of any minor crack.

By comparison, some use of failure criteria, or mechanical stimuli that bear some relation to the strength of bone, can be made to deal with a situation where there is some damage present in a microvolume of bone surrounded by completely healthy strong material. If we assume that repair is in response, not only to the stiffness of the material but also somehow to its residual load-bearing capacity, then the damaged tissue, although mechanically softer, will repair because it is also weaker. Mori & Burr (1993) who examined damage and remodelling in the legs of dogs caused by loading in three-point bending reported that they observed increased remodelling in the tensile side of the bone cortex compared to the compressive side despite the fact that the two sides had about the same amount of microcracking. Because microcracks tend to open as a result of tensile stresses and because strength in tension is less than strength in compression it may be that bone optimises its strength locally. The algorithms that would describe this case are not difficult to set up. In fact most failure criteria (except the Tsai-Wu) are 'normalized' versions of some distortional energy expression and therefore can be related to the von Mises stress. Also, lately, 'normalized' strain energy density criteria have appeared in order to predict the direction of development of macrocracks in composite anisotropic materials (Zhang *et al.* 1990). It seems therefore that there is a choice of algorithms that incorporate damage or strength in their expressions.

The relation between remodelling and microdamage is not clear, yet there is some evidence from the early work of Burr *et al.* (1985) that remodelling develops preferentially in fatigue-damaged regions. In a more recent report Mori & Burr (1993) addressed the question: does remodelling follow the accumulation of microcracks, or is it that microcracks accumulate at sites already under remodelling. They concluded that remodelling follows microcracking. This may be a result of either some modification of bone cell behaviour at the site of the microcrack that leads to the formation of new bone, or a result of some damage-related mechanical measure, which initiates remodelling. Indeed, the possibility exists that remodelling and microcracking are independent of each other and are a direct result of some mechanical measure. What is of paramount importance at the moment, as some have pointed out (Brown *et al.* 1990; Chen *et al.* 1994), is to establish clearly the nature of the mechanical stimulus and this inevitably requires both engineering and biological experiments. Once this is accomplished we will be more confident in discussing the whole issue of bone (re)modelling in relation to microcracking.

APPENDIX 1. ANISOTROPIC YIELD CRITERIA

Cezayirlioglu *et al.* (1985) suggested that anisotropic yield in bone can be described by either the Hill (1948) criterion:

$$F(\sigma_y-\sigma_z)^2+G(\sigma_z-\sigma_x)^2+H(\sigma_x-\sigma_y)^2+2L\tau_{yz}^2 +2M\tau_{zx}^2+2N\tau_{xy}^2=1, \quad \text{(A 1)}$$

(F, G, H, L, M and N are parameters), which for a transversely isotropic material and their test conditions (axial loads and torque) was reduced to:

$$2H\sigma_x^2+4N\tau_{xy}^2=1, \quad \text{(A 2)}$$

or the Tsai-Wu (1971) one, which from its general form:

$$F_i \sigma_i + F_{ij} \sigma_i \sigma_j = 1 \qquad \text{(A 3)}$$

was reduced in a similar manner to:

$$F_x \sigma_x + F_{xx} \sigma_x^2 + F_{ss} \tau_{xy}^2 = 1. \qquad \text{(A 4)}$$

APPENDIX 2. VON MISES STRESS

For a number of isotropic metals and polymers it has been observed that yield is apparently independent of the hydrostatic component of stress. Yield is then a function of the stress invariants (so called because they do not vary if one interchanges directions 1, 2 and 3) of the deviatoric stress tensor σ'_{ij} obtained by subtracting the hydrostatic components of stress from the total stress tensor. As a consequence the first form invariant

$$J'_1 = \sigma'_1 + \sigma'_2 + \sigma'_3 = 0. \qquad \text{(A 5)}$$

Von Mises (1913) suggested that in fact only the second invariant J'_2 has to be constant. There are three well known expressions of the von Mises criterion.

1. on the basis of the principal components of the total stress tensor:

$$\left.\begin{aligned} &(\sigma_1 - p)^2 + (\sigma_2 - p)^2 + (\sigma_3 - p)^2 = 2K^2 \\ &p = (1/3)\,(\sigma_1 + \sigma_2 + \sigma_3) \end{aligned}\right\} \qquad \text{(A 6)}$$

2. $$(\sigma_1 - \sigma_2)^2 + (\sigma_2 - \sigma_3)^2 + (\sigma_3 - \sigma_1)^2 = 6K^2 \qquad \text{(A 7)}$$

3. in relation to a Cartesian system of axes x, y, z (not the principal axes of stress)

$$(\sigma_{xx} - \sigma_{yy})^2 + (\sigma_{yy} - \sigma_{zz})^2 + (\sigma_{zz} - \sigma_{xx})^2 + 6(\sigma_{xy}^2 + \sigma_{yz}^2 + \sigma_{zx}^2) = 6K^2. \qquad \text{(A 8)}$$

On the basis of this criterion a von Mises stress (σ_{VM}) can be defined as a function of K. Mittlmeier *et al.* (1994) used $\sigma_{VM}^2 = 6K^2$. We chose the more common relation $2\sigma_{VM}^2 = 6K^2$ similar to Brown *et al.* (1990) and Chen *et al.* (1994).

The work reported here has been supported by a grant from the American Airforce Office for Scientific Research to study toughening mechanisms in mineralized tissues. The microscopical observations were carried out in the department of Biology of the University of St. Andrews Scotland. We thank Professor John Tucker, Dr M. Mogensen and John Mackie of the University of St. Andrews, for providing the Laser Scanning Confocal Microscope and helping in its operation. We are grateful to anonymous referees, and to Professor S. C. Cowin of the Department of Mechanical Engineering of the City University of New York, for a number of useful suggestions (including the title!) which improved this manuscript.

REFERENCES

Bonfield, W. & Datta, P.K. 1974 Young's modulus of compact bone. *J. Biomechan.* **7**, 147–149.

Brown, T.D., Pedersen, D.R., Gray, M.L., Brand, R.A. & Rubin, C.T. 1990 Toward an identification of mechanical parameters initiating periosteal remodeling: a combined experimental and analytic approach. *J. Biomechan.* **23**, 893–905.

Burr, D.B., Martin, R.B., Schaffler, M.B. & Radin, E.L. 1985 Bone remodeling in response to *in vivo* fatigue microdamage. *J. Biomechan.* **18**, 189–200.

Carter, D.R. 1987 Mechanical loading history and skeletal biology. *J. Biomechan.* **20**, 1095–1109.

Carter, D.R. & Wong, M. 1988 The role of mechanical loading histories in the development of diarthrodial joints. *J. Orthop. Res.* **6**, 804–816.

Carter, D.R., Fyhrie, D.P. & Whalen, R.T. 1987 Trabecular bone density and loading history: regulation of connective tissue-biology by mechanical energy. *J. Biomechan.* **20**, 785–794.

Carter, D.R., Orr, T.E. & Fyhrie, D.P. 1989 Relationships between loading history and femoral cancellous bone architecture. *J. Biomechan.* **22**, 231–244.

Carter, D.R., Wong, M. & Orr, T.E. 1991 Musculoskeletal ontogeny, phylogeny and functional adaptation. *J. Biomechan.* **24** (Suppl. 1), 3–16.

Cezayirlioglu, H., Bahniuk, E., Davy, D.T. & Heiple, K.G. 1985 Anisotropic yield behavior of bone under combined axial force and torque. *J. Biomechan.* **18**, 61–69.

Chen, J., Lu, X., Paydar, N., Akay, H.U. & Roberts, W.E. 1994 Mechanical simulation of the human mandible with and without an endosseous implant. *Med. Engng Phys.* **16**, 53–61.

Cowin, S.C. 1990 Deviatoric and hydrostatic mode interaction in hard and soft tissue. *J. Biomechan.* **23**, 11–14.

Cowin, S.C. 1993 Bone stress adaptation models. *J. Biomechan. Engng/Trans. ASME* **115**, 528–533.

Cowin, S.C. & Mehrabadi, M.M. 1989 Identification of the elastic symmetry of bone and other materials. *J. Biomechan.* **22**, 503–515.

Currey, J.D. 1984 Can strains give adequate information for adaptive bone remodeling? *Calcif. Tiss. Int.* **36**, S118–S122.

Currey, J.D. & Brear, K. 1974 Tensile yield in bone. *Calcif. Tiss. Res.* **15**, 173–179.

Currey, J.D. & Brear, K. 1992 Fractal analysis of compact bone and antler fracture surfaces. *Biomimetics* **1**, 103–118.

Currey, J.D., Brear, K. & Zioupos, P. 1994 Dependence of mechanical properties on fibre angle in Narwhal tusk, a highly oriented biological composite. *J. Biomechan.* **27**, 885–897.

Firoozbakhsh, K. & Cowin, S.C. 1981 An analytical model of Pauwels functional adaptation mechanism in bone. *J. Biomechan. Engng/Trans. ASME* **103**, 246–252.

Fisher, L. 1967 Optimization of orthotropic laminates. *J. Engng Indust./Trans. ASME* **89**, 399–402.

Frost, H.M. 1960 Presence of microscopic cracks *in vivo* in bone. *Henry Ford Hosp. Med. Bull.* **8**, 25–35.

Frost, H.M. 1973 *Bone modeling and skeletal modeling errors.* Springfield, Illinois, U.S.A.: Charles C. Thomas.

Frost, H.M. 1983 A determinant of bone architecture – the minimum effective strain. *Clin. Orthop. Relat. Res.* **175**, 286–292.

Fyhrie, D.P. & Carter, D.R. 1986 A unifying principle relating stress to trabecular bone morphology. *J. Orthop. Res.* **4**, 304–317.

Fyhrie, D.P. & Carter, D.R. 1990 Femoral head apparent density distribution predicted from bone stresses. *J. Biomechan.* **23**, 1–10.

Fyhrie, D.P. & Schaffler, M.B. 1994 Failure mechanisms in human vertebral cancellous bone. *Bone* **15**, 105–109.

Hayes, W.C. & Wright, T.M. 1977 An empirical strength theory for compact bone. *Fracture* **3**, 1173–1179.

Hill, R. 1948 A theory of the yielding and plastic flow of anisotropic metals. *Proc. R. Soc. Lond.* B **193**, 281–297.

Huiskes, R. & Hollister, S.J. 1993 From structure to process, from organ to cell: recent developments of FE-analysis in orthopaedic biomechanics. *J. Biomechan. Engng/Trans. ASME* **115**, 520–527.

Huiskes, R., Weinans, H. & van Rietbergen, B. 1993 Computer simulation of bone-remodelling processes around noncemented total hip replacements. In: *Recent advances in computer methods in biomechanics and biomedical engineering*. (ed. J. Middleton, G.N. Pande, K.R. Williams), pp. 8–19. Swansea: Books and Journals Int. Ltd.

Kachanov, L.M. 1958 On the time to failure under creep conditions. *Izv. Akad. Nauk. SSSR., Otd. Tekh. Nauk.* **8**, 26–31. (In Russian.)

Katz, J.L. & Meunier, A. 1987 The elastic anisotropy of bone. *J. Biomechan.* **20**, 1063–1070.

Lotz, J.C., Gerhart, T.N. & Hayes, W.C. 1991 Mechanical properties of metaphyseal bone in the proximal femur. *J. Biomech.* **24**, 317–329.

Martin, R.B. & Burr, D.B. 1989 *Structure, function, and adaptation of compact bone*. New York: Raven Press.

Mittlmeier, T., Mattheck, C. & Dietrich, F. 1994 Effects of mechanical loading on the profile of human femoral diaphyseal geometry. *Med. Engng Phys.* **16**, 75–81.

Mori, S. & Burr, D.B. 1993 Increased intracortical remodeling following fatigue damage. *Bone* **14**, 103–109.

Newaz, G.M. & Majumdar, B.S. 1992 Crack initiation around holes in a unidirectional MMC under fatigue loading. *Engng Fracture Mech.* **42**, 699–711.

Pope, M.H. & Outwater, J.O. 1974 Mechanical properties of bone as a function of position and orientation. *J. Biomechan.* **7**, 61–66.

Prendergast, P.J., McNamara, B.P. & Taylor, D. 1993 Prediction of bone adaptation based on accumulative damage and repair: finite element simulations. In: *Recent advances in computer methods in biomechanics and biomedical engineering*. (ed. J. Middleton, G.N. Pande, K.R. Williams), pp. 40–49, Swansea: Books and Journals Int. Ltd.

Prendergast, P.J. & Taylor, D. 1994 Prediction of bone adaptation using damage accumulation. *J. Biomechan.* **27**, 1067–1076.

Reilly, D.T. & Burstein, A.H. 1974 The mechanical properties of cortical bone. *J. Bone Joint Surg.* **56-A**, 1001–1022.

Reilly, D.T. & Burstein, A.H. 1975 The elastic and ultimate properties of compact bone tissue. *J. Biomechan.* **8**, 393–405.

Reilly, D.T., Burstein, A.H. & Frankel, V.H. 1974 The elastic modulus for bone. *J. Biomechan.* **7**, 271–275.

Rubin, C.T., McLeod, K.J. & Bain, S.D. 1990 Functional strains and cortical bone adaptation: epigenetic assurance of skeletal integrity. *J. Biomechan.* **23** (Suppl. 1), 43–54.

Saha, S. 1977 Longitudinal shear properties of human compact bone and its constituents, and the associated failure mechanisms. *J. Mater. Sci.* **12**, 1798–1806.

Smit, Th.H. & Schneider, E. 1994 The architecture of trabecular bone. In *Animal and cell abstracts*, p. 43. Swansea: Annual Meeting of the Society of Experimental Biology.

Tsai, S.W. & Wu, E.M. 1971 A general theory of strength for anisotropic materials. *J. Compos. Mater.* **5**, 58–80.

Tschantz, P. & Rutishauser, E. 1967 La surcharge méchanique de l'os vivant. Les déformations plastiques initiales et l'hypertrophie d'adaptation. *Ann. Anat. Path.* **12**, 223–248.

Turner, C.H., Forwood, M.R., Rho, J-Y. & Yoshikawa, T. 1994 Mechanical loading thresholds for lamellar and woven bone formation. *J. Bone Miner. Res.* **9**, 87–97.

Van der Meulen, M.C., Beaupré, G.S. & Carter, D.R. 1993 Mechanobiologic influences in long-bone cross-sectional growth. *Bone* **14**, 635–642.

Viano, D. 1986 Biomechanics of bone and tissue: a review of material properties and failure characteristics. In *Biomechanics & medical aspects of lower limb injuries*, **P-186**, pp. 33–63. San Diego, California: Proceedings of the Society of Automotive Engineers.

Von Mises, R. 1913 Mechanik der festen Körper im plastisch-deformablen Zustand. *Nachr. Ges. Wiss. Göttingen.* 582–592.

Zhang, S.Y., Tsai, L.W. & Liu, J.Q. 1990 Strain-energy density ratio criterion for fracture of composite-materials. *Engng Fracture Mechan.* **37**, 881–889.

Zioupos, P. & Currey, J.D. 1994 The extent of micro-cracking and the morphology of microcracks in damaged bone. *J. Mater. Sci.* **23**, 978–986.

Zioupos, P., Currey, J.D. & Sedman, A.J. 1994 An examination of the micromechanics of failure of bone and antler by acoustic emission tests and Laser scanning confocal microscopy. *Med. Engng Phys.* **16**, 203–212.

Received 25 August 1994; accepted 26 October 1994

PHILOSOPHICAL TRANSACTIONS OF THE ROYAL SOCIETY B BIOLOGICAL SCIENCES

(*a*)

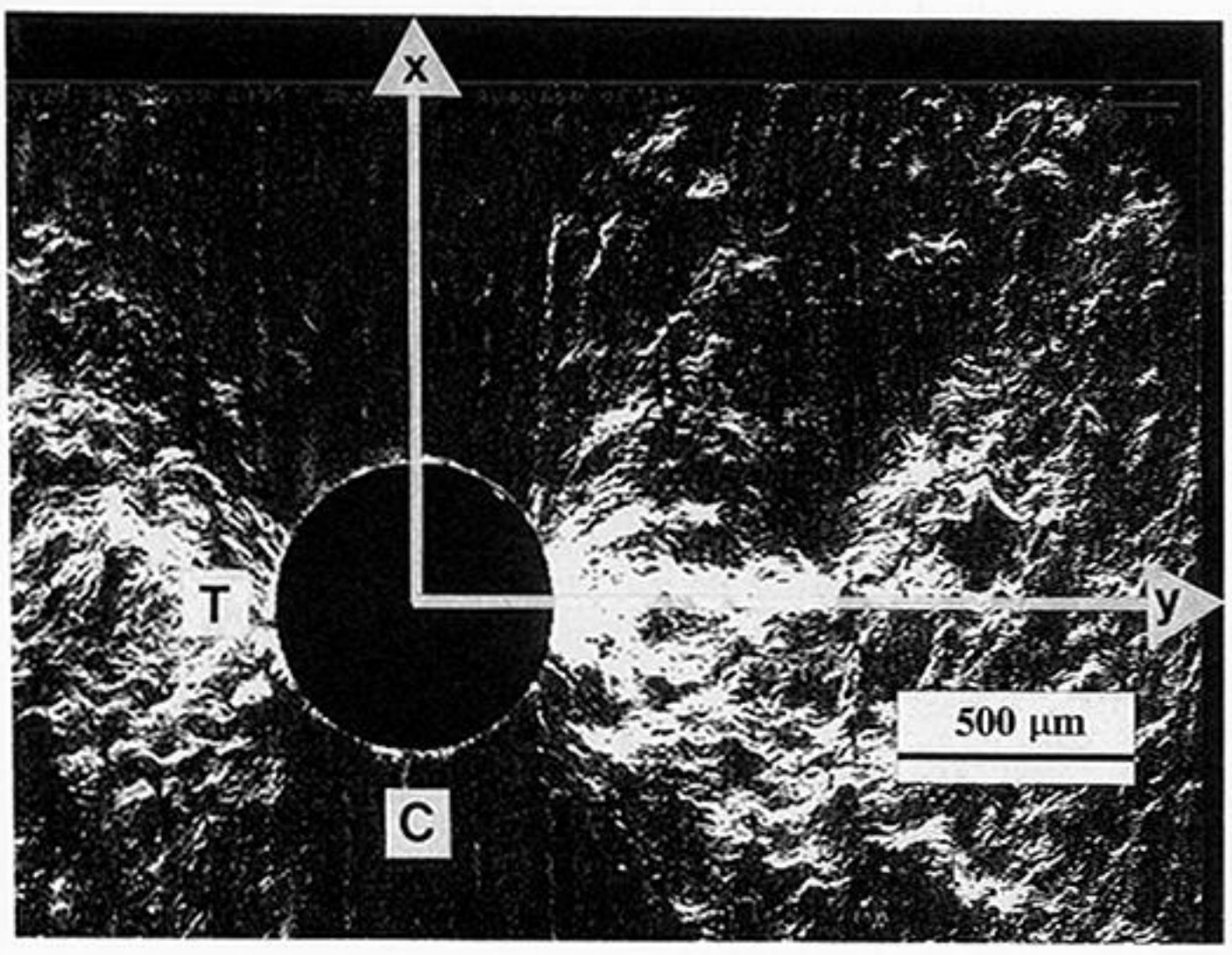

(*b*)

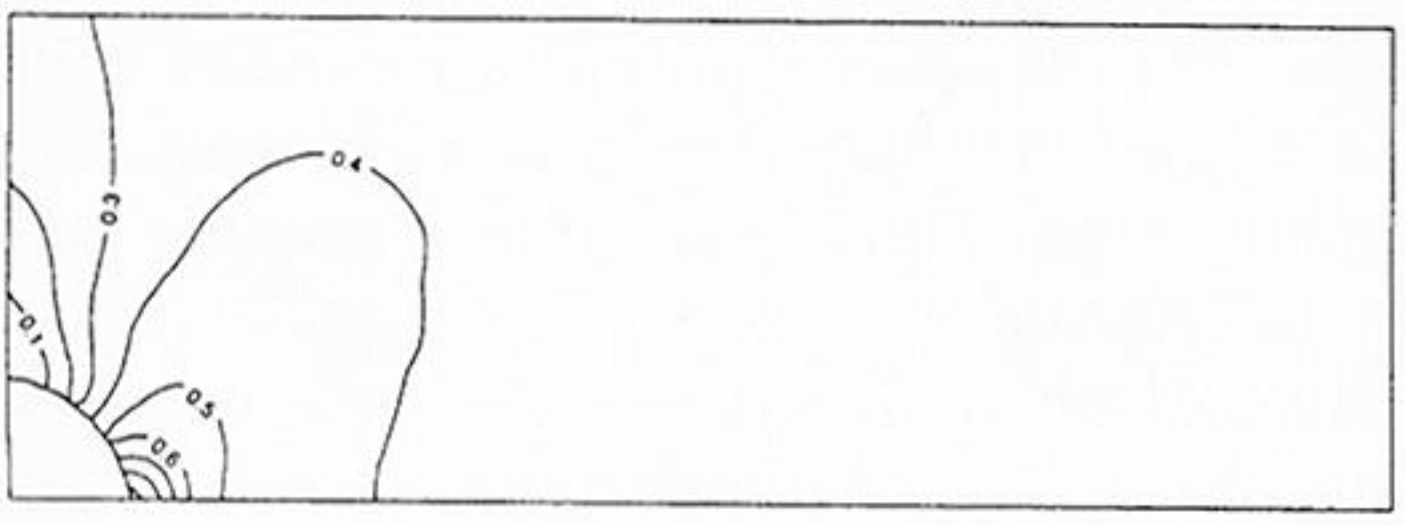

(*c*)

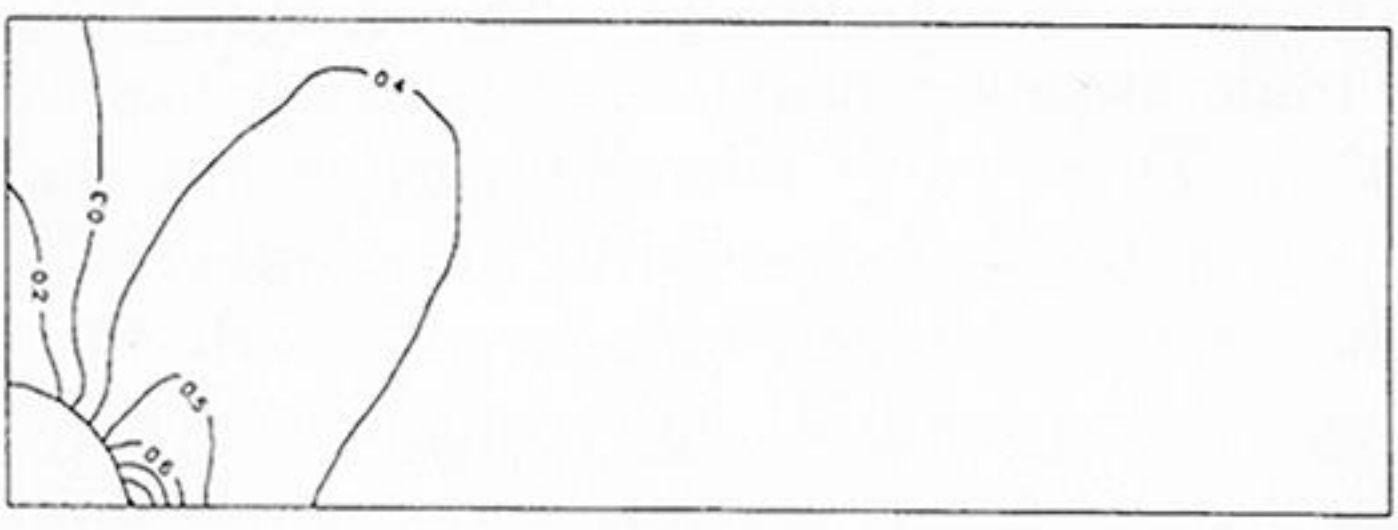

(*d*)

(*e*)

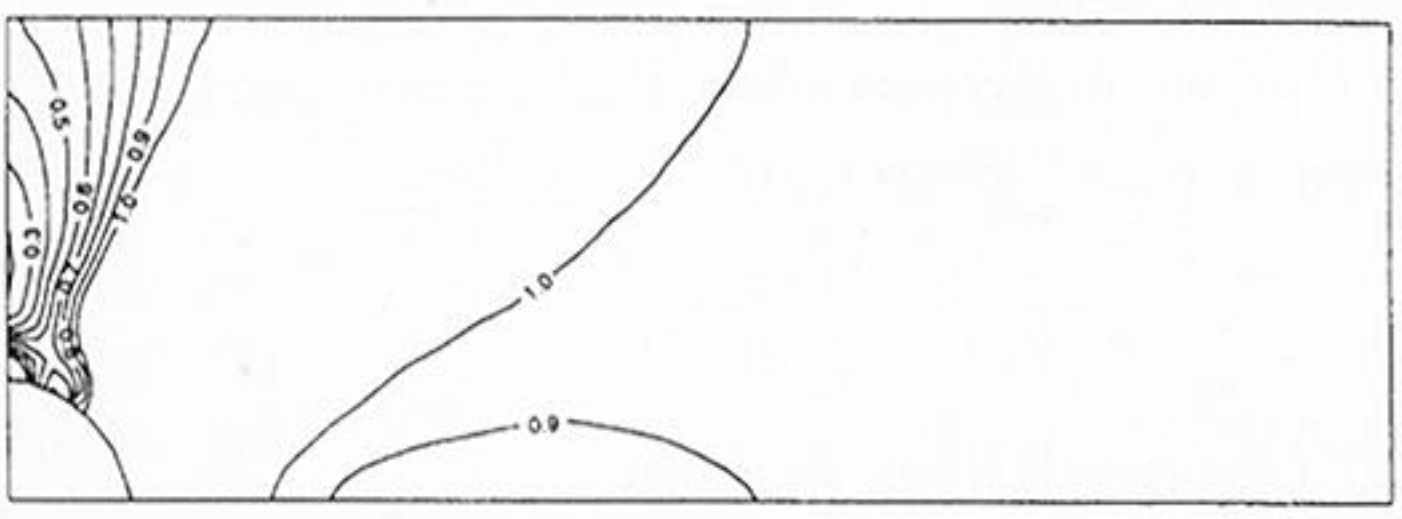

(*f*)

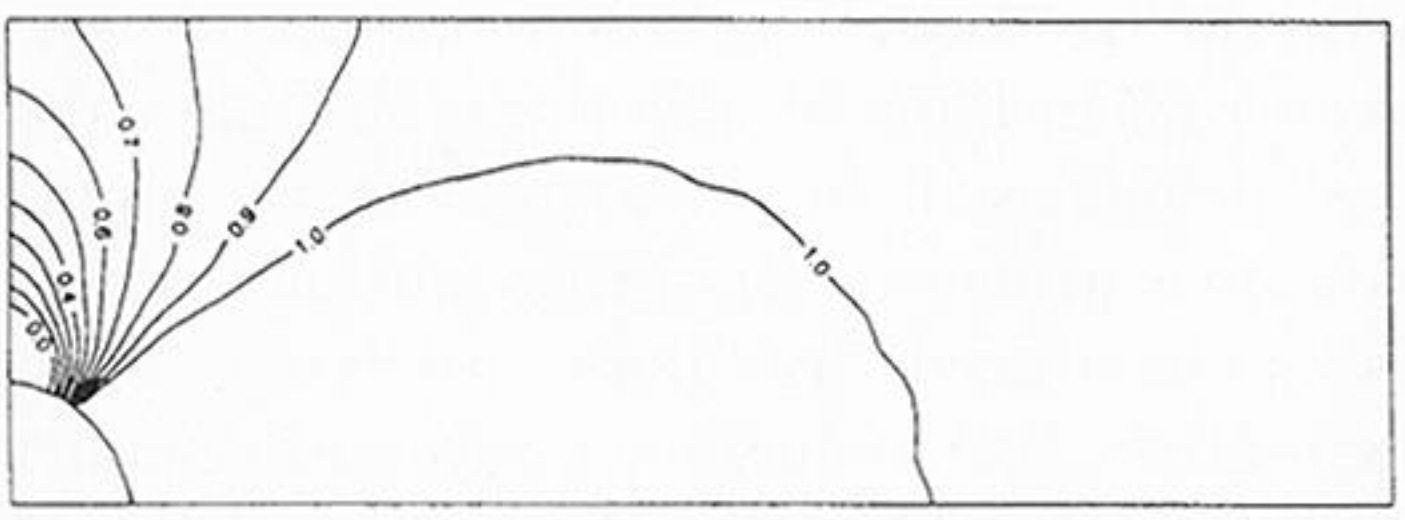

igure 4. (*a*) microcracking around a 550 μm diameter hole specimen number 54; tension is applied in the *x*-direction. Microcracks appear readily in regions under tension (T) ompared to regions under compression (C). (*b*) pattern of ormalized maximum principal stress: (*c*) pattern of ormalized von Mises stress; (*d*) pattern of normalized SED;) yield contours for the Hencky-von Mises criterion; (*f*) ield contours for the Tsai-Wu criterion. The yield contours f value 1 are in effect a boundary where the material starts yield; no account is taken of the fact that because of the ield, the original elastic stress may be redistributed and transmitted.

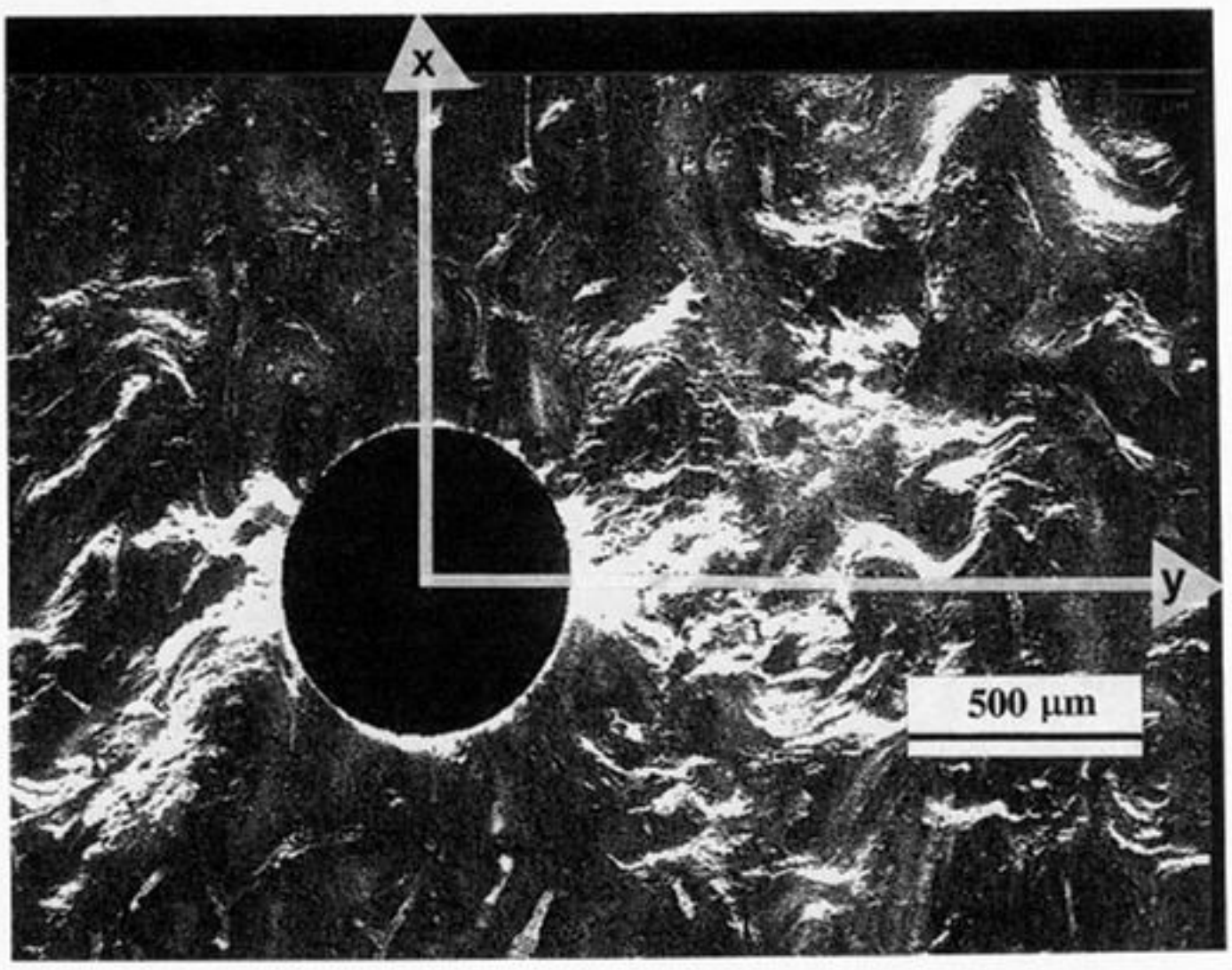

(*a*)

(*b*)

(*c*)

(*d*)

(*e*)

(*f*)

gure 5. (*a*) microcracking around a 550 μm diameter hole specimen number 11; (*b*) pattern of normalized maximum incipal stress; (*c*) pattern of normalized von Mises stress;) pattern of normalized SED; (*e*) yield contours for the encky-von Mises criterion; (*f*) yield contours for the Tsai-u criterion.

(*a*)

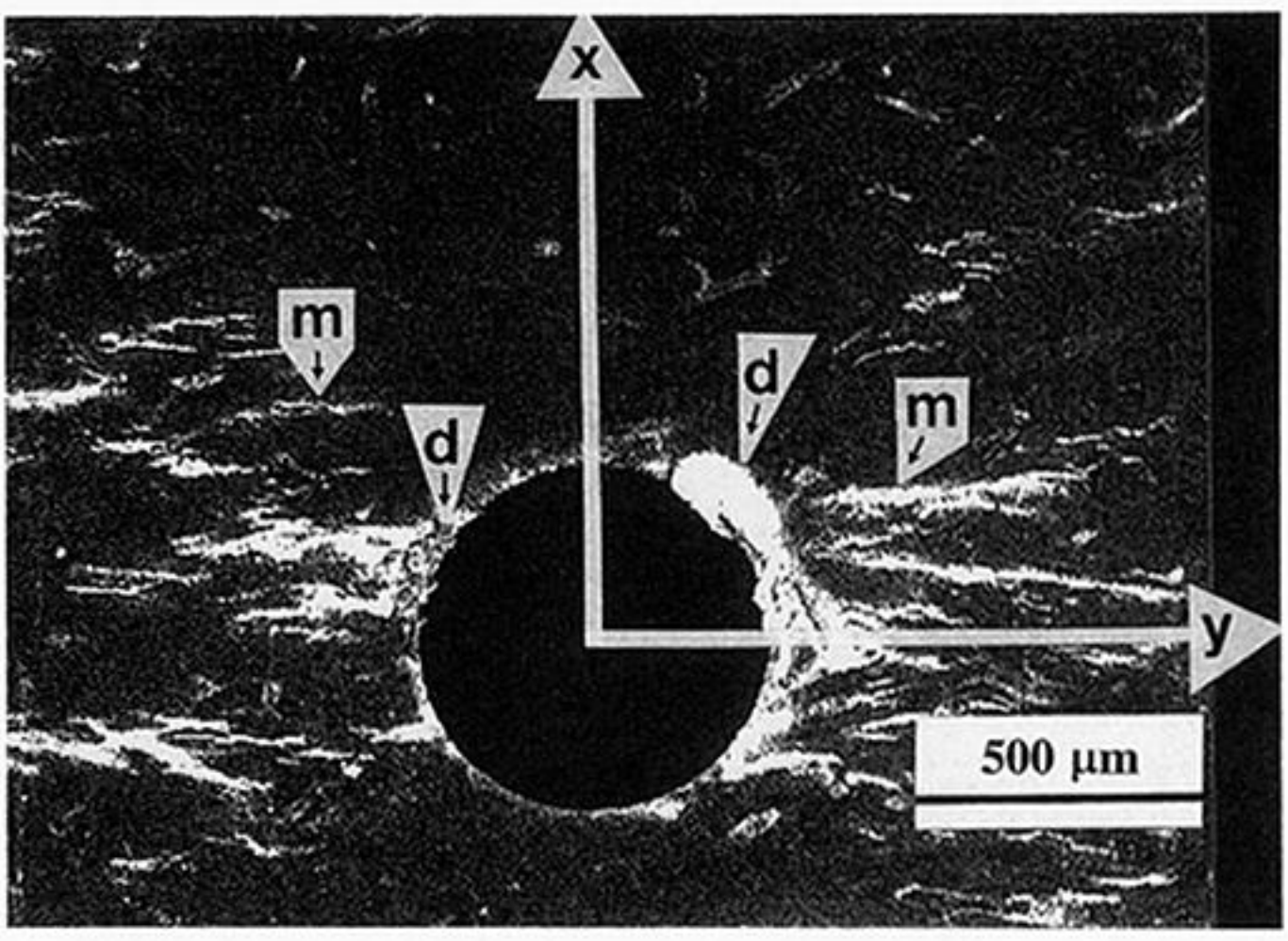

(*b*)

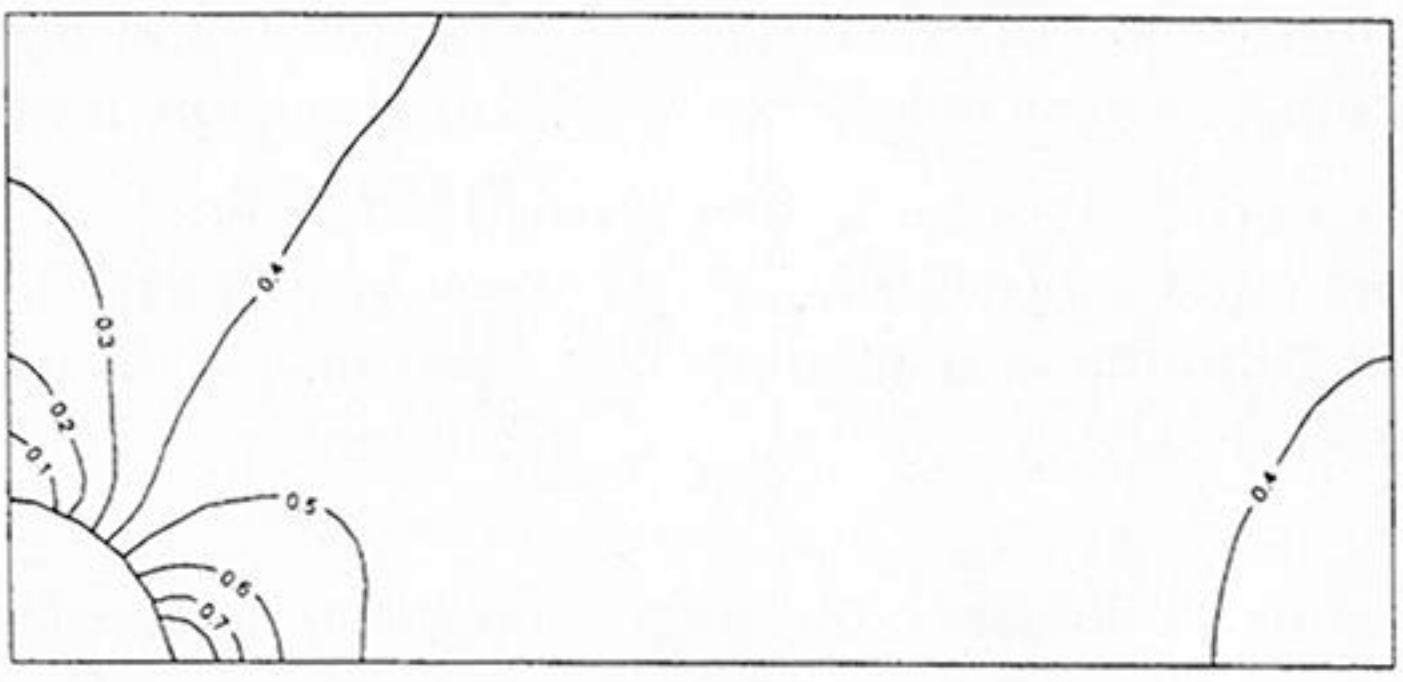

(*c*)

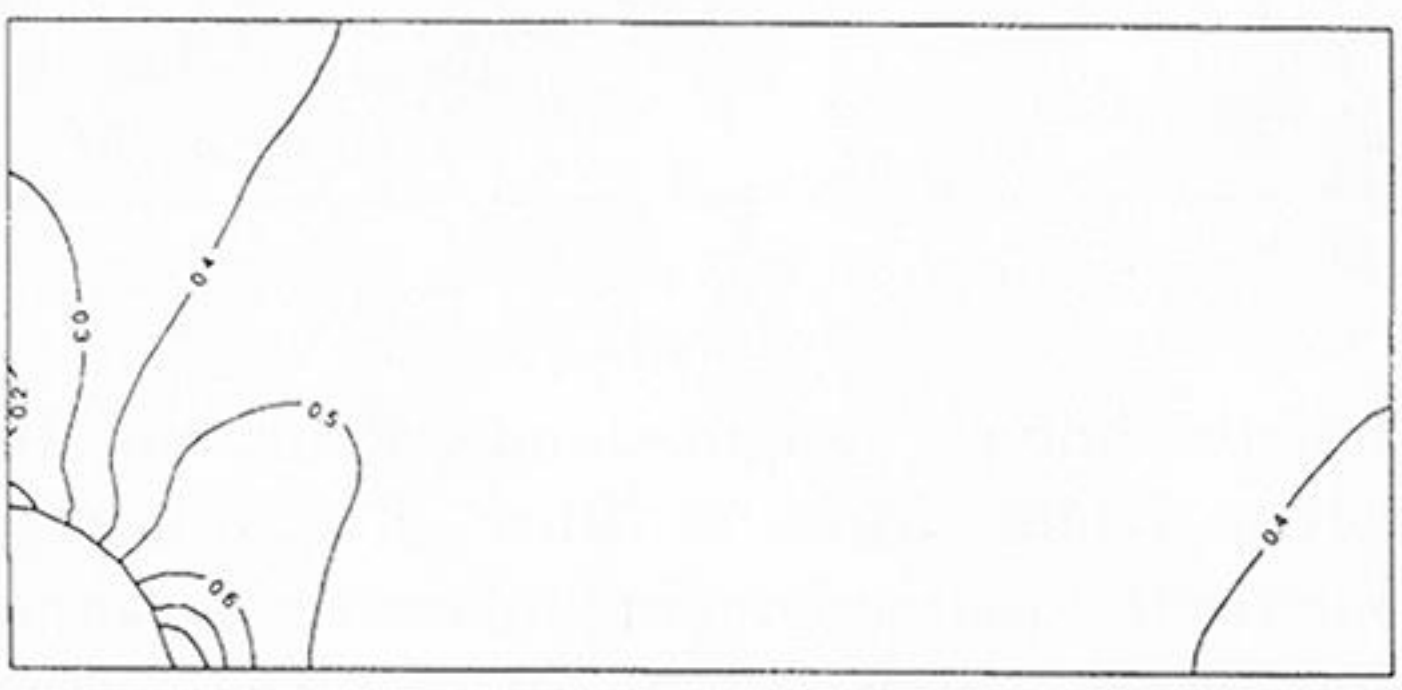

(*d*)

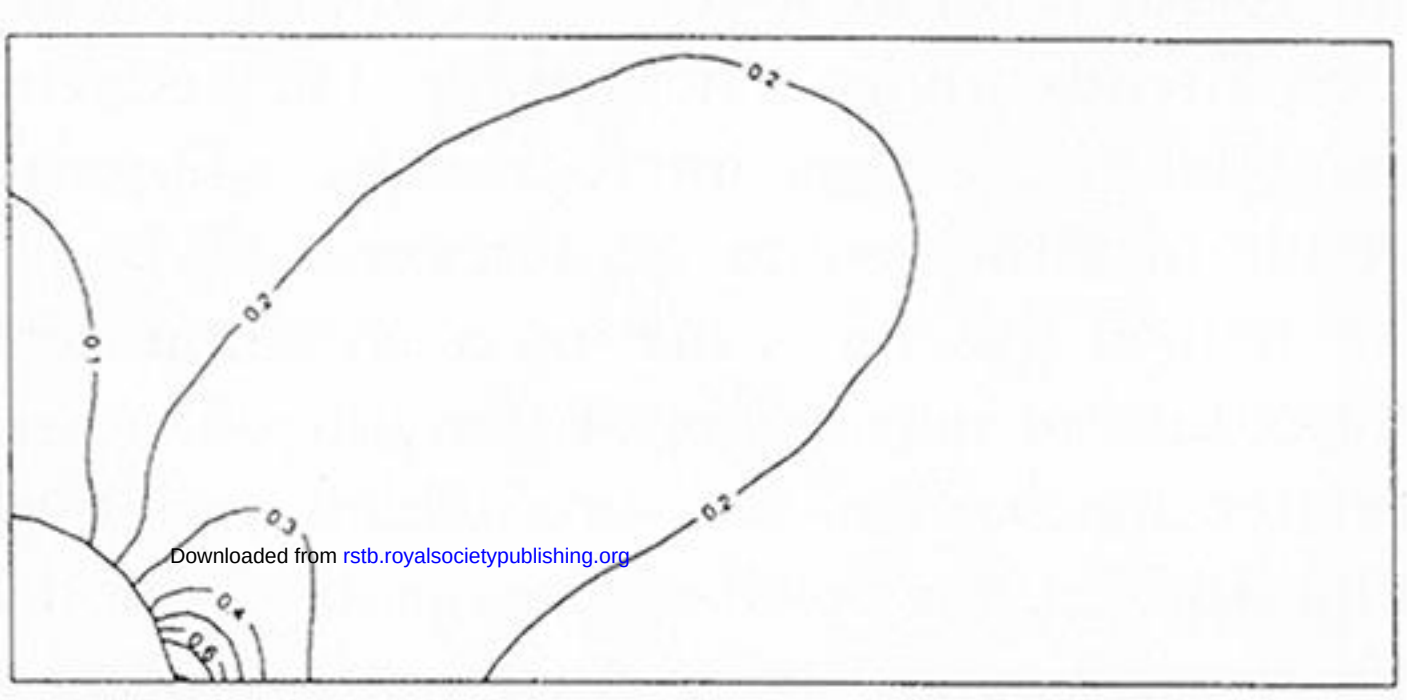

(*e*)

(*f*)

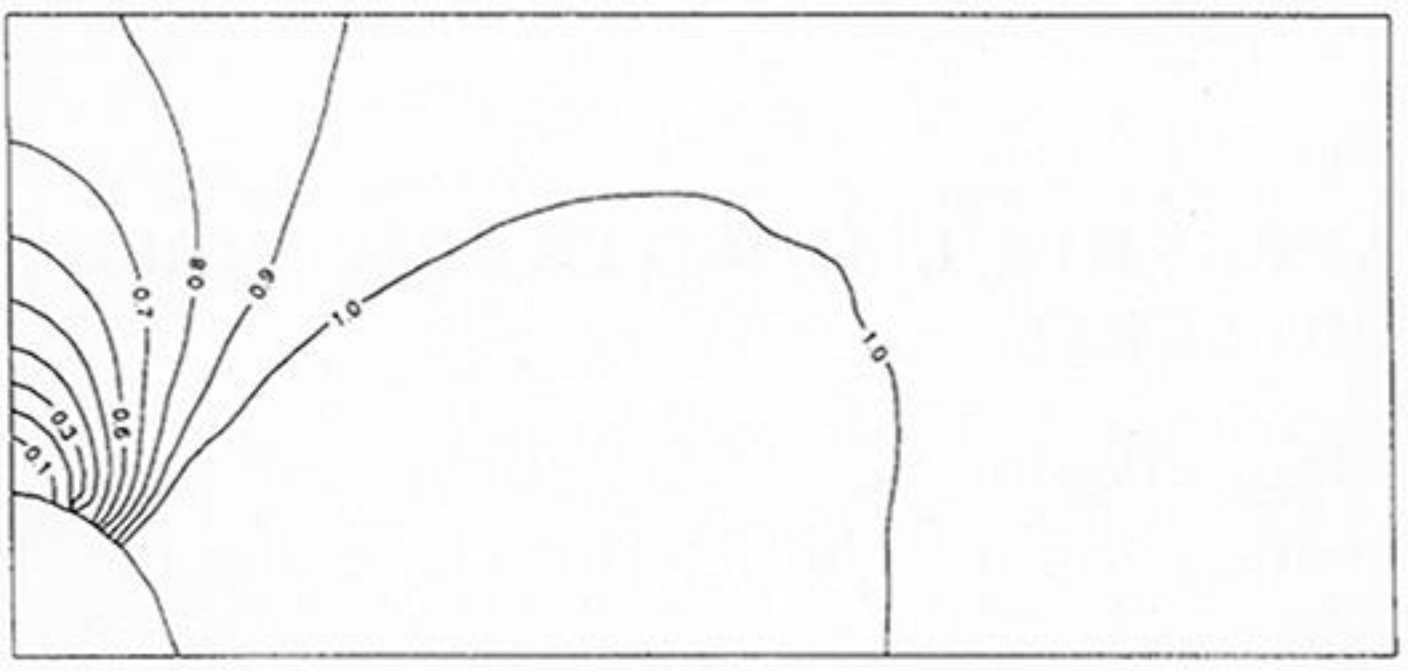

gure 6. (*a*) microcracking around a 550 μm diameter hole specimen number 12; (*b*) pattern of normalized maximum incipal stress; (*c*) pattern of normalized von Mises stress;) pattern of normalized SED; (*e*) yield contours for the encky-von Mises criterion; (*f*) yield contours for the Tsai- u criterion. Note that at the microscale cracks (m) open ostly along the weak direction. Some damage caused by a ght eccentricity of the drill during the preparation can be en near the hole (d).